(12)

construction engineering research laboratory

United States Army
Corps of Engineers
...Serving the Army
...Serving the Nation

Technical Report M-307
March 1982

EVALUATION OF APPLICABILITY OF STANDARD CW EMI/RFI SHIELDING EFFECTIVENESS TEST TECHNIQUES TO ASSESSMENT OF EMP HARDNESS OF TACTICAL SHELTERS

AD A113042

DTIC FILE COPY

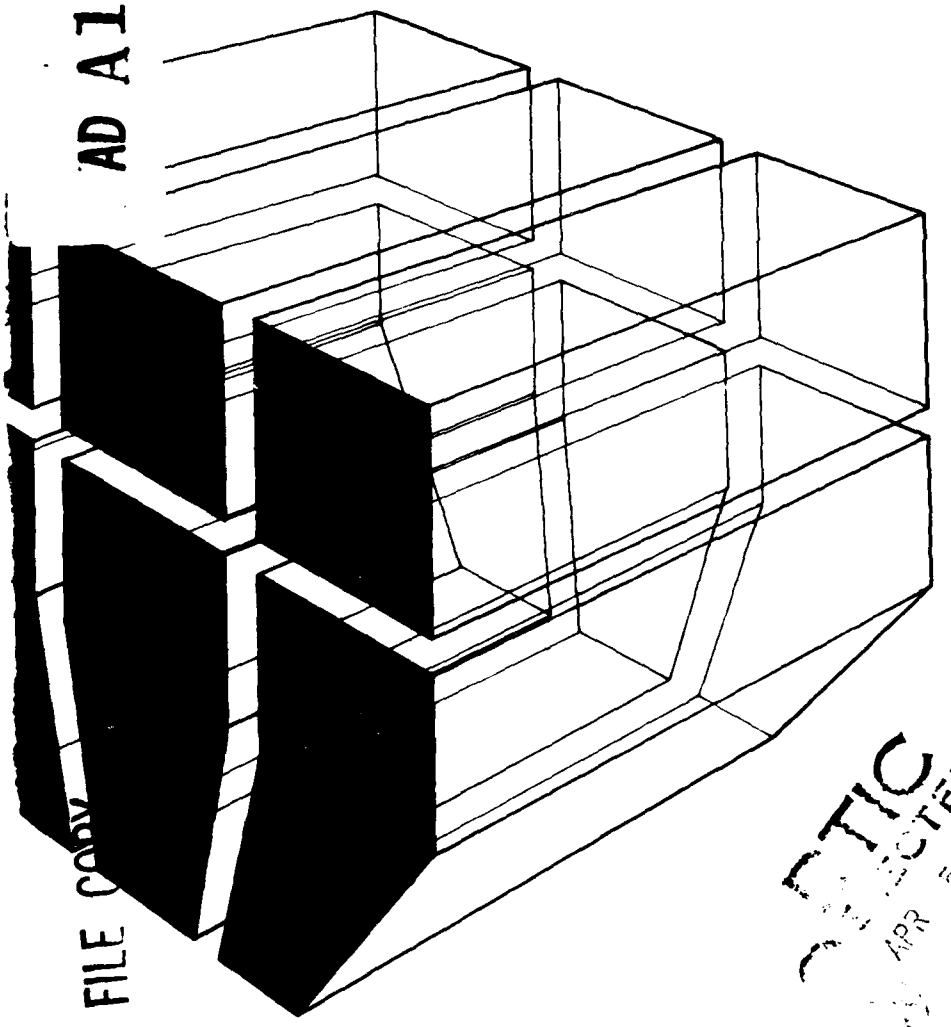

by
Roy Axford
Ray McCormack
Raj Mittra

DTIC
ELECTE
APR 5 1982
D

CERL

Approved for public release; distribution unlimited.

The contents of this report are not to be used for advertising, publication, or promotional purposes. Citation of trade names does not constitute an official indorsement or approval of the use of such commercial products. The findings of this report are not to be construed as an official Department of the Army position, unless so designated by other authorized documents.

DESTROY THIS REPORT WHEN IT IS NO LONGER NEEDED
DO NOT RETURN IT TO THE ORIGINATOR

UNCLASSIFIED

SECURITY CLASSIFICATION OF THIS PAGE *(When Data Entered)*

REPORT DOCUMENTATION PAGE		READ INSTRUCTIONS BEFORE COMPLETING FORM
1. REPORT NUMBER CERL-TR-M-307	2. GOVT ACCESSION NO. AD-A113 042	3. RECIPIENT'S CATALOG NUMBER
4. TITLE *(and Subtitle)* EVALUATION OF APPLICABILITY OF STANDARD CW EMI/RFI SHIELDING EFFECTIVENESS TEST TECHNIQUES TO ASSESSMENT OF EMP HARDNESS OF TACTICAL SHELTERS		5. TYPE OF REPORT & PERIOD COVERED FINAL 6. PERFORMING ORG. REPORT NUMBER
7. AUTHOR(s) Roy Axford Ray McCormack Raj Mittra		8. CONTRACT OR GRANT NUMBER(s) MIPR FY76208100019 Project ESD/OCR-3
9. PERFORMING ORGANIZATION NAME AND ADDRESS U.S. ARMY CONSTRUCTION ENGINEERING RESEARCH LABORATORY P.O. Box 4005, Champaign, IL 61820		10. PROGRAM ELEMENT, PROJECT, TASK AREA & WORK UNIT NUMBERS
11. CONTROLLING OFFICE NAME AND ADDRESS		12. REPORT DATE March 1982 13. NUMBER OF PAGES 57
14. MONITORING AGENCY NAME & ADDRESS*(if different from Controlling Office)*		15. SECURITY CLASS. *(of this report)* Unclassified 15a. DECLASSIFICATION/DOWNGRADING SCHEDULE

16. DISTRIBUTION STATEMENT *(of this Report)*

Approved for public release; distribution unlimited.

17. DISTRIBUTION STATEMENT *(of the abstract entered in Block 20, if different from Report)*

18. SUPPLEMENTARY NOTES

Copies are obtainable from the National Technical Information Service
Springfield, VA 22161

19. KEY WORDS *(Continue on reverse side if necessary and identify by block number)*

shelters
electromagnetic shielding
radiation hardening

20. ABSTRACT *(Continue on reverse side if necessary and identify by block number)*

This report investigates the validity of analytical techniques for converting continuous wave (CW) test data to values for electromagnetic pulse (EMP) to measure the EMP hardness of tactical shelters. MIL-STD-285 and specifications for CW testing IEEE 299 specify measurements in the near field using dipole and loop antennas. Consequently, the test wavefronts are spherical, rather than planar, as in the case of an EMP. Thus, correction factors for EMP needed to be developed.

DTIC
ELECTE
APR 5 1982
S D
H

DD FORM 1 JAN 73 1473 EDITION OF 1 NOV 65 IS OBSOLETE

UNCLASSIFIED

SECURITY CLASSIFICATION OF THIS PAGE *(When Data Entered)*

Block 20 continued.

Two methods documented in the literature were analyzed: (1) the Schelkunoff transmission line theory approach and its extension to slotted shields, and (2) the plane wave spectrum approach as used to calculate the shielding effectiveness of a multiple-layer shield to the fields of a loop antenna positioned in the coaxial configuration. It was found that extension of the transmission line theory approach to slotted shields yielded inaccurate results, especially for loop antennas. However the plane wave spectrum approach, when combined with Huygen's principle, yields results that are in good agreement with experimental results.

The results of this investigation have produced recommendations for CW test techniques for evaluating EMP hardness of tactical shelters. These are:

1. Use specifications listed in IEEE 299, with modifications as given in the Air Force report ESL-TR-80-01.

2. Make maximum use of the IEEE 299 large-loop test or seam leak detectors.

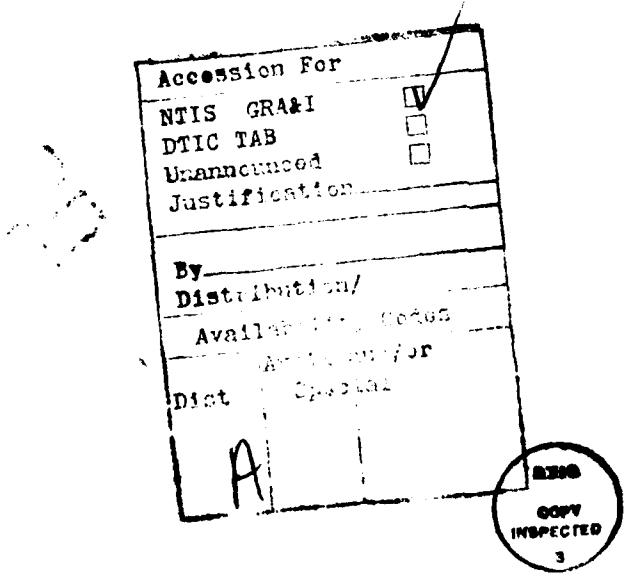

EXECUTIVE SUMMARY

Electromagnetic fields are classified as magnetic, plane, or electric according to the ratio of their magnetic and electric field components. This ratio is a prime factor in determining the degree to which a field will be reduced by an electromagnetic shield. Within the electromagnetic pulse (EMP) spectrum (100 Hz to 100 MHz for a high-altitude nuclear burst), it is easier for a tactical shelter to shield against a plane wave field than a magnetic field; it is also easier to shield against an electric field than a plane wave field. The fields caused by a high-altitude nuclear burst are plane wave fields. The standard currently used to verify the EMP hardness of tactical shelters (MIL-STD-285) specifies shielding effectiveness measurements with magnetic and electric fields within the frequency spectrum of an EMP. Consequently, shielding effectiveness measurements made on a tactical shelter according to MIL-STD-285 will only give upper and lower bounds on the shelter's EMP shielding effectiveness. The spread between these bounds is about 100 dB in the EMP spectrum. Furthermore, the upper bound provided by electric field measurements is often greater than the dynamic range of the measuring equipment.

The problems associated with applying MIL-STD-285 to assessing the EMP hardness of shielded enclosures were first addressed in the literature by Monroe in 1973.* Monroe applied the transmission line theory of shielding and developed correction factors for MIL-STD-285 shielding effectiveness measurements to convert them to values meaningful for EMP plane wave fields. The only other literature to address this problem (Villaseca in 1977**) evaluated the validity of Monroe's work from an analytical standpoint. Villaseca found no technical errors in Monroe's work within the stated assumptions; however, he did object to Monroe's application of transmission line theory to the shielding of the near fields of loop and monopole antennas (the magnetic and electric field test antennas, respectively, specified in MIL-STD-285). Villaseca derived correction factors for MIL-STD-285 measurements that are based on plane wave spectrum theory—a more rigorous analytical approach than transmission line theory. These correction factors agreed with Monroe's within practical limits. Neither Monroe nor Villaseca experimentally verified their correction factors.

The objective of this research was to apply Monroe's and Villaseca's analytical techniques to problems that could be modeled easily in CERL's electromagnetics laboratory. Two shielding models of geometries encountered in tactical shelters were examined: slotted shields and multiple-layered shields. Computer programs were developed to predict the shielding of these structures for the fields of MIL-STD-285 test antennas. A computer code using the transmission line theory outlined in Monroe's report was written for the slotted shield. This code was used to predict the shielding that was measured on two slotted shields in the laboratory with loop and monopole antennas. Reasonable agreement between predicted and experimental results was achieved for monopole antennas; however, agreement for loop antennas was not acceptable. Further computer modeling was done using the "Dipole-Moment Approximation" for loop antennas. Improved correlation between predicted and measured results was obtained for loops in both the coplanar and coaxial test orientations.

Formulations based on the plane wave spectrum approach were used in a computer program to calculate the shielding effectiveness of multiple-layered shields for the fields of a loop antenna in the coaxial test configuration. The shielding predicted by the program

*R. L. Monroe, *EMP Shielding Effectiveness and MIL-STD-285*, HDL-TR-1636/AD771997 (Harry Diamond Laboratories, U.S. Army Materiel Command, July 1973).

**E. Villaseca, C. Davis, W. Blackwood, and W. Getson, *An Investigation of the Validity of Applying MIL-STD-285 to EMP Shielding Effectiveness*, ADA051889, prepared by Harris Corp. Electronics System Division (Defense Nuclear Agency, 15 April 1977).

was compared with measurements taken in the laboratory on dual-layer, copper-foil shields mounted in an aperture in a steel-construction shielded room. When the effects of this aperture were accounted for with a separate computer program, agreement with experimental results was excellent.

Direct experimental evaluation of the applicability of MIL-STD-285 to the assessment of the EMP hardness of tactical shelters could not be made in this study. However, at this time, the best techniques for testing a tactical shelter's shielding effectiveness are application of the procedures outlined in MIL-STD-285 and in IEEE 299, along with the guidelines presented in this report. Particular attention must be paid to electromagnetic leakage at discontinuities in the shield panels, such as seams, door seals and cable entries. Also, test frequencies outside the EMP spectrum may need to be specified, depending on the mission of the shelter.

FOREWORD

This investigation was performed for the Electronic Systems Division, Shelter Management Office, Hanscom AFB, MA, under MIPR FY76208100019, Project ESD/OCR-3. The ESD/OCR-3 project officer was LT Steve Penaskovic.

The study was done by the Engineering and Materials Division (EM), U.S. Army Construction Engineering Research Laboratory (CERL). CERL personnel directly involved in the study were Mr. R. G. McCormack, Mr. R. A. Axford, Jr., and Dr. Paul Sonnenburg. Dr. Raj Mittra is with University of Illinois' Electromagnetics Laboratory.

Dr. Robert Quattrone is Chief of EM. COL Louis J. Circeo is Commander and Director of CERL, and Dr. L. R. Shaffer is Technical Director.

CONTENTS

FIGURES

EVALUATION OF APPLICABILITY OF STANDARD CW EMI/RFI SHIELDING EFFECTIVENESS TEST TECHNIQUES TO ASSESSMENT OF EMP HARDNESS OF TACTICAL SHELTERS

1 INTRODUCTION

Background

The accepted technique for determining the electromagnetic pulse (EMP) hardness of a shielded enclosure or tactical shelter is to subject it to a threat-level pulse environment. This is generally not a practical solution, however, because EMP simulation equipment is expensive. MIL-STD-285[1] and IEEE 299[2] list the radio frequency, continuous wave (CW) test techniques agreed on by shielding manufacturers and by personnel who accept shielded enclosures. The measurements specified by these standards are made in the near field using dipole and loop antennas. Consequently, the test wavefronts impinging on the shielded enclosure are spherical, rather than planar, as in the case of an EMP. Specifically, the wave impedance of the test wavefronts will be above and below, respectively, that of the EMP planewave for the dipole and loop fields. Thus, the shielding effectiveness measured by the dipole and loop tests will be above and below that of an incident EMP.

Monroe[3] has proposed extension of the Shelkunoff transmission line theory and Villaseca[4] has proposed use of the plane wave spectrum approach in an attempt to develop correction factors for converting MIL-STD-285 measurements to values meaningful for EMP planar radiation. However, knowledge of these efforts is not widespread, and the results have not been applied to the procurement of shielded facilities. Furthermore, little experimental work has been done to verify the correction factors.

The military currently has no CW test techniques to directly measure the EMP hardness of tactical shelters; furthermore, there has been no experimental verification of previous efforts to convert existing accepted standard CW measurements to values meaningful for EMP. Therefore, the U.S. Army Construction Engineering Research Laboratory (CERL) was requested to examine the validity of the analytical techniques used to convert CW test data to values for EMP.

Objective

The objectives of this study were to: (1) examine the validity of the EMP correction factors for MIL-STD-285 measurements developed by Monroe and Villaseca, and (2) recommend CW test procedures for verifying EMP hardness of tactical shelters.

Approach

A literature search was conducted to provide information on previous work done to provide EMP correction factors for MIL-STD-285 measurements (Chapter 2). Computer programs were used to calculate the shielding effectiveness predicted by analytical models for slotted shields and multiple-layer shields. Laboratory experiments were then carried out to verify the results of these computer programs (Chapters 3 and 4). The effects of cavity resonances on tactical shelters were investigated (Chapter 5). CW test procedures for verifying EMP hardness of tactical shelters were recommended, based on the results of the research (Chapter 6).

Mode of Technology Transfer

It is anticipated that this study will impact on the application of the radio frequency interference (RFI) shielding effectiveness measurement techniques specified in MIL-STD-285, IEEE 299, and NSA 65-6 for the EMP hardness testing of GLCM control electronics modules.

2 SUMMARY OF CORRECTION FACTORS DEVELOPED FOR EMP

Cost constraints and the nonavailability of portable EMP simulators often make full-scale, threat-level EMP hardness testing of shielded facilities and tactical shel-

[1] *Military Standard Attenuation Measurements for Enclosures, Electromagnetic Shielding for Electronic Test Purposes, Method of,* MIL-STD-285 (Department of Defense, 25 June 1956).

[2] *Proposed IEEE Recommended Practice for Measurement of Shielding Effectiveness of High-Performance Shielding Enclosures,* IEEE 299 (Institute of Electrical and Electronics Engineers [IEEE], June 1969).

[3] R. L. Monroe, *EMP Shielding Effectiveness and MIL-STD-285,* HDL-TR-1636/AD771997 (Harry Diamond Laboratories, U.S. Army Materiel Command, July 1973).

[4] E. Villaseca, C. Davis, W. Blackwood, and W. Getson, *An Investigation of the Validity of Applying MIL-STD-285 to EMP Shielding Effectiveness,* ADA051889, prepared by Harris Corp. Electronics System Division (Defense Nuclear Agency, 15 April 1977).

ters impossible. Usually, a threat-level pulse test would be considered only for initial acceptance or design evaluation testing. CW shielding effectiveness test techniques offer economical alternatives to pulse tests for EMP hardness testing of production shelter units and for periodic maintenance testing.

MIL-STD-285 specifies the test procedures most often used to measure the electromagnetic shielding effectiveness of shielded enclosures. IEEE 299 outlines similar procedures with additional tests for seam leakage (large loop tests). Within the generally accepted frequency spectrum of an EMP caused by a high-altitude nuclear burst (100 Hz to 100 MHz), the procedures specified in MIL-STD-285 and IEEE 299 call for use of loop and monopole antennas as radiating sources for the measurements. These give shielding effectiveness measurements for low-impedance (magnetic) and high-impedance (electric) fields, respectively. The wave impedance of a high-altitude EMP impinging on a tactical shelter will be 377 Ω, which lies between the wave impedances of the loop and monopole sources at the specified measurement distances, and within the EMP spectrum. Thus, the question is what information the standard test procedures of MIL-STD-285 and IEEE 299 can give about the EMP shielding effectiveness of tactical shelters.

The problem of applying MIL-STD-285 test procedures to evaluating the EMP shielding effectiveness of shielded enclosures was first considered by Monroe in EMP Shielding Effectiveness and MIL-STD-285[5]. Monroe employs Schelkunoff's transmission line theory approach to shielding to address the fact that the mismatch between the intrinsic impedance of the shielding material and the wave impedance of the impinging radiation is critical to a structure's shielding effectiveness. This fact is apparent in the standard transmission line theory equation for shielding effectiveness:

$$SE = R + A + B \quad (dB) \qquad [Eq\ 1]$$

where:

$R = 20 \log \frac{|k+1|^2}{4|k|}$, initial reflection loss

$A = 8.686\ \alpha t$, attenuation loss in penetrating shield once

$B = 20 \log \left| 1 - \frac{(k-1)^2}{(k+1)^2} e^{-2(1+j)\alpha t} \right|$, losses due to multiple reflections within the shield

$k = \frac{Z_{wave}}{Z_{shield}}$, impedance ratio of shield and impinging wave

$\alpha = (\pi \mu \sigma f)^{1/2}$, reciprocal of shield skin depth

$Z_{shield} = \left(\frac{j 2\pi f \mu}{\sigma} \right)^{1/2}$

f = frequency

t = shield thickness

μ = shield permeability

σ = shield conductivity

$j = \sqrt{-1}$

The term corresponding to the initial reflection loss, R, depends directly on the ratio of the impinging wave impedance to the intrinsic impedance of the shield.

Monroe observes that MIL-STD-285 measurements made with loops and monopoles give lower and upper bounds, respectively, on a shielding enclosure's EMP shielding effectiveness at a given frequency. This is because the impedance mismatch between a loop source, an EMP (plane wave), a monopole (or dipole) source, and the intrinsic impedance of a shield is ordered as:

$$1 < \left| \frac{Z_{loop}}{Z_{shield}} \right| < \left| \frac{Z_{EMP}}{Z_{shield}} \right| < \left| \frac{Z_{monopole}}{Z_{shield}} \right| \qquad [Eq\ 2]$$

The spread between the theoretical bounds given by loop and monopole measurements can be about 100 dB in the frequency region below 1 MHz. Thus, a structure's actual EMP shielding effectiveness cannot be accurately estimated directly from MIL-STD-285 measurements alone. (Furthermore, neither MIL-STD-285 or IEEE 299 specify both loop and monopole tests at any given frequency.)

Monroe has evaluated the transmission line expressions for the difference between the shielding of a given conductor to an EMP and to a loop source (or, equivalently between an EMP and a monopole [dipole] source); he then gives a correction factor $\delta(f)$ which can be added to a loop measurement or sub-

[5] R. L. Monroe, *EMP Shielding Effectiveness and MIL-STD-285*, HDL-TR-1636/AD771997 (Harry Diamond Laboratories, U.S. Army Materiel Command, July 1973).

tracted from a monopole measurement to estimate the shelter's EMP shielding effectiveness:

$$\delta(f) = SE_{EMP} - SE_{loop} = 20 \log\left(\frac{Z_{EMP}}{|Z_{loop}|}\right) \qquad \text{[Eq 3]}$$

$$= SE_{monopole} - SE_{EMP} = -20 \log\left(\frac{Z_{EMP}}{|Z_{monopole}|}\right)$$

where: $Z_{EMP} = 377\ \Omega$

Thus, $\delta(f)$ can be evaluated at the test frequency for the appropriate source and added to the MIL-STD-285 test result in order to estimate the structure's actual EMP shielding effectiveness.

The validity of Monroe's work is addressed by Villaseca.[6] This study acknowledges that Monroe's work was the first step in applying standard EMI shielding effectiveness measurement techniques to the EMP problem. It concludes that, within the stated assumptions, there are no technical errors in the solution presented. However, Villaseca disagrees with the underlying assumption on which the report is based. Monroe's application of the transmission line theory of shielding inherently assumes that a plane wave is incident upon the shielding material. However, Villaseca points out that this assumption is not true for the actual situation in the MIL-STD-285 test setup, since the shield is in the extreme near field of the test antennas. When the source antenna is placed close to the shield, the incident waves are of a complex spherical nature, rather than planar.

Villaseca derives correction factors for MIL-STD-285 measurements via an independent technique, free of any simplifying assumptions; this technique uses the concept of an "Angular Spectrum of Plane Waves." Introduced by Booker and Clemmou[7] in 1957, the concept allows the representation of an antenna's radiation pattern by a linear combination of plane waves. The steady-state radiation pattern of the antenna reduces to an angular spectrum of these plane waves taken over all angles. The portions of the pattern function that correspond to complex angles determine the reactive, nonpropagating energy stored in the near field of the antenna. The transmission line approach used by Monroe does not allow consideration of the reactive energy which, in the near field, is relatively large compared to the real, propagating, energy. Villaseca states that the reactive coupling of energy is of fundamental importance in the problems associated with shielding effectiveness measurements made in the near field with low-level CW sources.

In the plane wave spectrum approach, an electromagnetic field ($\underline{E}$ or $\underline{H}$) is expanded in a set of plane waves as:

[Eq 4]

$$\underline{E}(x, y, z) = \int_{-\infty}^{\infty}\int_{-\infty}^{\infty} \underline{E}(K_x, K_y) e^{-j(K_x x + K_y y + K_z z)} dK_x\, dK_y$$

where:

$\underline{E}(K_x, K_y)$ = the plane wave spectrum or density of the electric field per square wave number

$\underline{K} = K_x \hat{x} + K_y \hat{y} + K_z \hat{z}$ is the propagation vector.

From Maxwell's equations, it follows that

$$|\underline{K}| = \beta = \frac{2\pi}{\lambda} \qquad \text{[Eq 5]}$$

which implies that

$$K_z = \sqrt{\beta^2 - (K_x^2 + K_y^2)} \qquad \text{[Eq 6]}$$

As shown by Eq 6, the (K_x, K_y) plane can be divided into two regions separated by a circle centered at the origin of radius β. The inner part of the circle, corrresponding to real values of K_z, defines the propagating portion of the plane wave spectrum and is called the "visible" region. The outer part of the circle, called the "invisible" region, corresponds to imaginary values of K_z and defines the non-propagating, evanescent waves which are exponentially attenuated for $z>0$.

In short, Villaseca's approach derives transmission coefficients for the visible and invisible portions of transverse magnetic (TM) and transverse electric (TE) plane wave power spectrum expansions for dipole and loop test antennas, respectively. Then, the shielding effectiveness of a plane shield is determined by calculating the ratio of the power transmitted through the shield to the power incident on the shield in both the visible and invisible regions of the spectrum. The same

[6]E. Villaseca, C. Davis, W. Blackwood, and W. Getson, *An Investigation of the Validity of Applying MIL-STD-285 to EMP Shielding Effectiveness*, ADA051889, prepared by Harris Corp. Electronics System Division (Defense Nuclear Agency, 15 April 1977).

[7]H. G. Booker and P. L. Clemmou, *Proceedings of IEEE*, Vol 97, Part III (1957), pp 11-17.

calculations are also performed for a uniform plane wave incident on the shield in order to produce correction factors applicable to MIL-STD-285 measurements. Villaseca found that if the calculations were confined to the visible region, correction factors agreed precisely with those of Monroe. Including the contribution of the power in the invisible region, produced a loop correction factor about 10 dB greater and a dipole correction factor about 10 dB less than Monroe's.

The plane wave spectrum technique provided correction factors that did not agree precisely with those derived by the transmission line technique; however, Villaseca concluded that Monroe's report represented a good engineering approximation for the case of a uniform conductivity shield with no apertures or seams. He cautions, however, against the application of Monroe's approach to shields with penetrations or seams.

In summary, two basic approaches have been used to obtain correction factors for converting MIL-STD-285 loop and monopole (dipole) shielding effectiveness measurements to values meaningful for an incident EMP (plane waves). The Schelkunoff transmission line approach used by Monroe represents a first-order approach to the problem and is considered to be a reasonable approximation only for a uniform planar shield. As shown in Chapter 3, the extension of Monroe's approach to slotted shields does not always yield accurate results.

The plane wave spectrum concept used by Villaseca is a more rigorous and versatile analytical approach for calculating shielding effectiveness. Since it does not rely on any simplifying assumption, it holds great promise for application to general classes of shielding problems. Chapter 4 discusses the application of plane wave spectrum techniques to calculating the shielding effectiveness of double-layered shields when illuminated by a loop antenna in the coaxial orientation. Appendix A presents an application of plane wave spectrum techniques to calculating the shielding effectiveness of a multiple-layer shield when illuminated by arbitrary fields.

3 SHIELDING EFFECTIVENESS OF SLOTTED SHIELDS

The narrow slot is a common analytical model for discontinuities in practical shielded enclosures such as welds and door seams. In the present context, a narrow slot is one whose length is much larger than its width. This discussion is limited to slots that are electrically small; i.e., one whose length is much smaller than the wavelengths of the impinging radiation.

Monroe[8] extends the Schelkunoff transmission line theory of shielding to the calculation of the shielding effectiveness of a perfectly conducting shield containing an electrically small, narrow slot. Based on the assumption that the illuminating radiation will be approximately uniform, Monroe states (without further justification) that the shielding effectiveness due to reflection from the slot can be expressed as:

$$SE = 20 \log \frac{|k+1|^2}{4|k|} \qquad \text{[Eq 7]}$$

where: $k = \frac{Z_{wave}}{Z_{slot}}$

and Z_{slot} = impedance of the slot.

This equation has exactly the same form as the reflection term in the expression for the shielding effectiveness of a planar shield with no discontinuities. For a slotted shield, the intrinsic impedance of the shielding material has been replaced by the slot impedance.

The slot impedance is highly dependent on the polarization of the incident field. Maximum coupling through the slot is obtained when the incident electric field vector is aligned in a direction perpendicular to the large dimension of the slot. For this polarization, the slot impedance is related to the driving point impedance, Z_{cd}, of the complementary dipole and is given by Monroe as:

$$Z_{slot} = \frac{\eta^2}{4 Z_{cd}} = \frac{\eta^2}{4} \frac{R_{cd} - jX_{cd}}{R_{cd}^2 + X_{cd}^2} \qquad \text{[Eq 8]}$$

where:

$\eta = 377\ \Omega$

R_{cd} = real part of Z_{cd}

X_{cd} = imaginary part of Z_{cd}

[8] R. L. Monroe, *EMP Shielding Effectiveness and MIL-STD-285*, HDL-TR-1636/AD771997 (Harry Diamond Laboratories, U.S. Army Materiel Command, July 1973).

Approximate expressions for R_{cd} and X_{cd} are cited by Monroe as:

$$R_{cd} = \frac{Z_o}{Z} \frac{\sinh(2\gamma)}{\cosh^2(\gamma) - \cos^2(\beta L)} \qquad \text{[Eq 9]}$$

$$X_{cd} = \frac{Z_o}{Z} \frac{\sin(2\beta L)}{\cosh^2(\gamma) - \cos^2(\beta L)} \qquad \text{[Eq 10]}$$

where:

$$Z_o = 120\left[\ln\left(\frac{L}{a}\right) - \frac{1}{2}\ln\left(\frac{2L}{\lambda}\right) - 1\right]$$

$$\gamma = \frac{2 R_{ad}}{Z_o}$$

$$R_{ad} = 15\ \{[2 + 2\cos(2\beta L)]\ S_1(2\beta L) - \cos(2\beta L)\ S_1(4\beta L) - 2\sin(2\beta L)\ S_i(2\beta L) + \sin(2\beta L)\ S_i(4\beta L)\}$$

$$S_1(x) = \int_o^x \frac{1 - \cos(s)}{s}\, ds$$

$$S_i(x) = \int_o^x \frac{\sin(s)}{s}\, ds$$

2L = length of slot

2a = width of slot

An examination of the behavior of the slot impedance with frequency indicates that within the EMP spectrum, the shielding effectiveness of a slotted shield is approximately constant with frequency for the fields produced by a loop source. The shielding of the fields produced by a dipole or monopole by a slotted shield shows about a 40-db/decade decrease with increasing frequency.

CW testing was conducted on slotted shield panels in the laboratory to examine the accuracy of the transmission line theory of shielding when applied to slots. Two 1/4-in. thick aluminum panels, one with a 1-meter by 1/8-in. slot and the other with a 1/2-meter by 1/16-in. slot, were mounted over a 2- x 4-ft test aperture in a steel shielded room. The panels were tested in the MIL-STD-285 configuration with 12-in. loop and 41-in. monopole antennas over the frequency band from 100 kHz to 300 MHz. To compare the predictions of the transmission line theory to the experimental data, Eqs 7 through 10 were programmed on a CDC 7600 computer via the FORTRAN program SLOT (see Appendix B). Shielding effectiveness values for loop and monopole sources located 1 ft away from the shield were calculated for both slot sizes. Experimental data were taken with the loop antennas oriented in the coplanar position with the plane of the antennas perpendicular to the slot's long dimension. Data for the monopoles were taken with the antennas oriented perpendicular to the slot. These antenna orientations provided an incident field with the electric field vector oriented in a direction perpendicular to the slot's long dimension.

Figures 1 and 2 present the experimental results, along with the transmission line theory predictions, for the shielding effectiveness of the slotted panels to the monopole fields for both slot sizes. As shown in the figures, the transmission line theory predictions are within an average of 6 dB of the measured values, for the larger slot, while the predictions for the smaller slot show about a 14 dB underestimate of shielding effectiveness.

Figures 3 and 4 compare the transmission line theory predictions of shielding effectiveness for loop antennas in the coplanar orientation and show experimental measurements. For this source and orientation, the transmission line theory predictions underestimate the shielding effectiveness of the slotted panel by about 14 and 18 dB for the larger and smaller slots, respectively. Thus, for loops in the coplanar orientation (a common method for checking seam leakage), the slot impedance shielding model does not appear to give accurate results.

C. M. Butler[9] suggests an alternate method for calculating the shielding effectiveness of a perfectly conducting shield with an electrically small, narrow slot. The technique, known as the "Dipole-Moment Approximation," allows the expression of the electromagnetic fields that penetrate an electrically small aperture in terms of the fields of equivalent electric

[9]C. M. Butler, "Dipole Moment Approximation and Polarizabilities," Section 2.1.3.2 in *EMP Interaction Principles, Techniques, and Reference Data*, EMP Interaction 2-1, AFWL-TR-80-402 (Air Force Weapons Lab, Air Force Systems Command, December 1980).

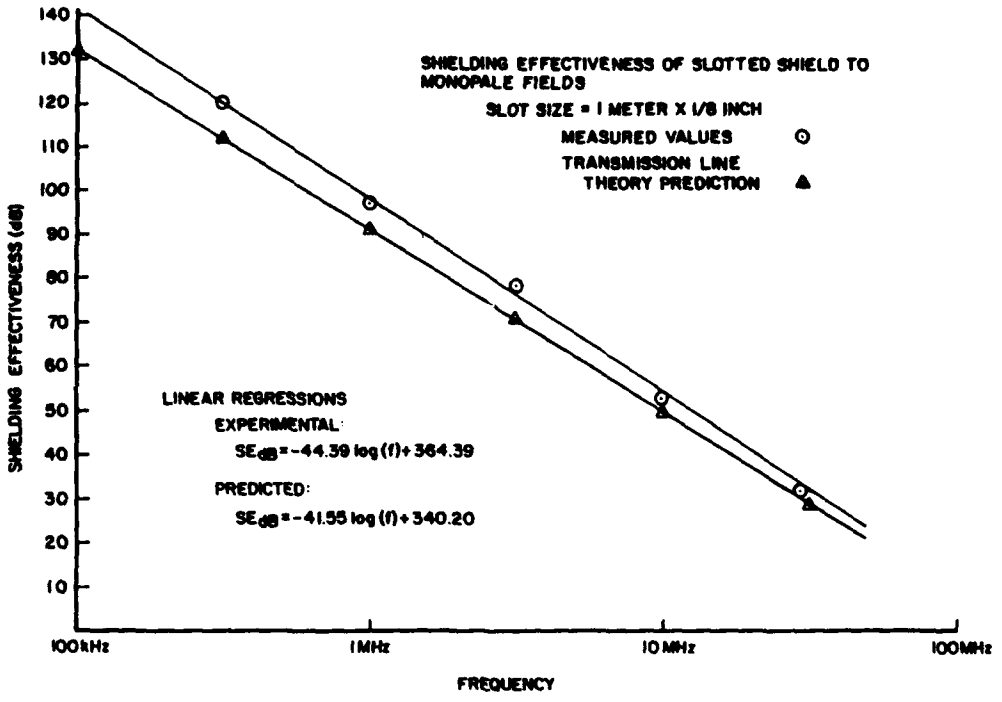

Figure 1. Shielding effectiveness of slotted shield to monopole fields. Slot size = 1 m X 1/8 in.

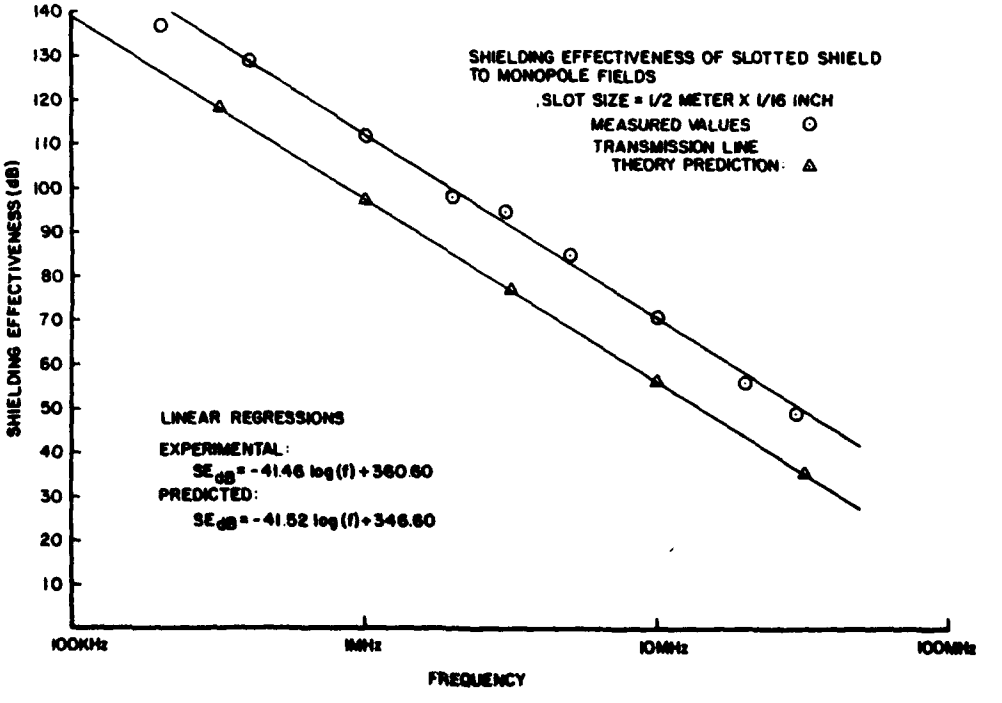

Figure 2. Shielding effectiveness of slotted shield to monopole fields. Slot size = 1/2 m X 1/16 in.

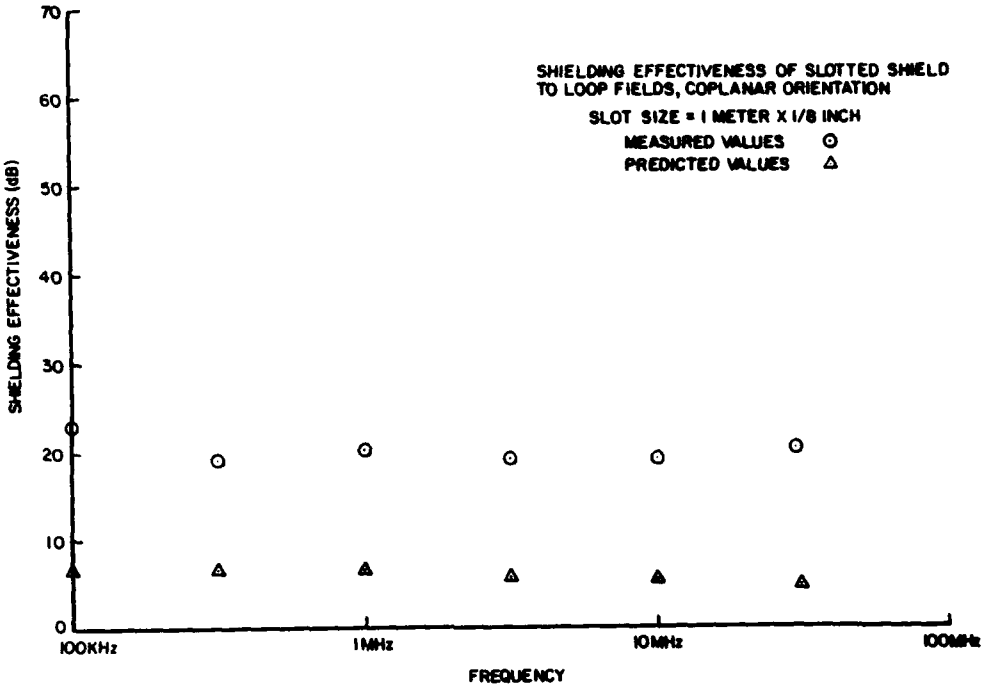

Figure 3. Shielding effectiveness of slotted shield to loop fields, coplanar orientation. Slot size = 1 m X 1/8 in.

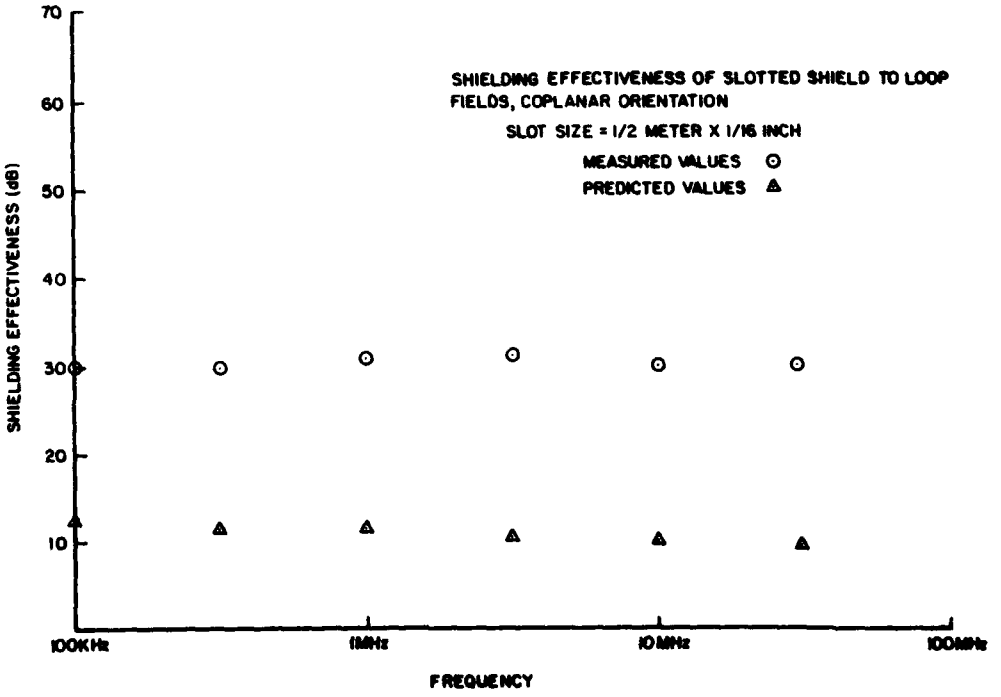

Figure 4. Shielding effectiveness of slotted shield to loop fields, coplanar orientation. Slot size = 1/2 m X 1/16 in.

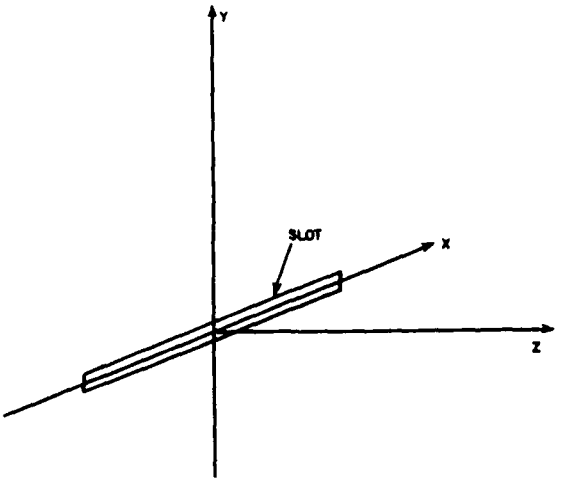

Figure 5. Orientation of slot in cartesian coordinate system.

and magnetic dipoles in the aperture. These dipoles can be expressed in terms of the fields incident on the aperture. The remainder of this discussion will be confined to the shielding of the fields of loop antennas that are positioned in both the coplanar and coaxial orientations. Consequently, only the magnetic field propagating from the aperture will be considered.

The magnetic field, $\vec{H}^d$, radiated by an electric dipole, $\vec{p}_a$, and a magnetic dipole, $\vec{m}_a$, located at the origin of a cartesian coordinate system in free space, is given by:

$$\vec{H}^d(\vec{r}, s) = -s\,\vec{p}_a(s) \times \vec{\nabla} G(\vec{r}, s) - \vec{\nabla} \times [\vec{m}_a(s) \times \vec{\nabla} G(\vec{r}, s)] \qquad \text{[Eq 11]}$$

where:

$$G(\vec{r}, s) = e^{-j\frac{2\pi}{\lambda} r}/4\pi r$$

λ = wavelength

The aperture equivalent electric and magnetic dipoles, $\vec{p}_a$ and $\vec{m}_a$, are given in terms of the electric and magnetic polarizability tensors, $\overleftrightarrow{\alpha}_e$ and $\overleftrightarrow{\alpha}_m$, by:

$$\vec{p}_a = 2\,\overleftrightarrow{\alpha}_e \cdot \vec{E}_{sc}, \quad \vec{m}_a = -2\overleftrightarrow{\alpha}_m \cdot \vec{H}_{sc} \qquad \text{[Eq 12]}$$

where:

$\vec{E}_{sc}$, $\vec{H}_{sc}$ are the short circuit fields in the aperture (equal to two times incident fields)

$\overleftrightarrow{\alpha}_e$ and $\overleftrightarrow{\alpha}_m$ are two-dimensional symmetric dyads.

The components of the polarizability tensors for a narrow slot oriented in a cartesian coordinate system as shown in Figure 5 are given on page 437 of Butler.[10] Calculations for the slot dimensions used in this study yield

$$\alpha_{m,\,xx} = 2.132 \times 10^{-2} >> 1.979 \times 10^{-6} = \alpha_{e,\,zz} = \alpha_{m,\,yy}$$

for the 1-meter by 1/8-in. slot and

$$\alpha_{m,\,xx} = 2.665 \times 10^{-3} >> 2.474 \times 10^{-7} = \alpha_{e,\,zz} = \alpha_{m,\,yy}$$

for the 1/2-meter by 1/16-in. slot. Thus, the contribution to the magnetic field $\vec{H}^d$ by the electric dipole is negligible, and Eq 11 reduces to

$$\vec{H}^d(\vec{r}, s) = -\vec{\nabla} \times [\vec{m}_a(s) \times \vec{\nabla} G(\vec{r}, s)] \qquad \text{[Eq 13]}$$

where only the $\alpha_{m,\,xx}$ component of $\overleftrightarrow{\alpha}_m$ is non-zero. Thus, $\vec{m}_a$ is given by

$$\vec{m}_a = -4\,\alpha_{m,\,xx}\,H_{inc,\,x}\,\hat{x} \qquad \text{[Eq 14]}$$

where:

$H_{inc,\,x}$ is the x-component of the magnetic field incident on the aperture. Letting

$$m_x = -4\,\alpha_{m,\,xx}\,H_{inc,\,x} \qquad \text{[Eq 15]}$$

[10] C. M. Butler, "Dipole Moment Approximation and Polarizabilities," Section 2.1.3.2 in *EMP Interaction Principles, Techniques, and Reference Data*, EMP Interaction 2-1, AFWL-TR-80-402 (Air Force Weapons Lab, Air Force Systems Command, December 1980).

and substituting into Eq 7 yields

$$\vec{H}^d(r) = \left(m_x \frac{\partial^2}{\partial y^2} \frac{e^{-jkr}}{4\pi r} + m_x \frac{\partial^2}{\partial x^2} \frac{e^{-jkr}}{4\pi r}\right)\hat{x} + \left(-m_x \frac{\partial^2}{\partial x \partial y} \frac{e^{-jkr}}{4\pi r}\right)\hat{y} + \left(-m_x \frac{\partial^2}{\partial x \partial z} \frac{e^{-jkr}}{4\pi r}\right)\hat{z} \qquad \text{[Eq 16]}$$

Referring to the coordinate system shown in Figure 5, the components of $\vec{H}^d$ of interest are H_z^d for the coaxial orientation and H_x^d for the coplanar orientation.

The derivatives indicated in Eq 16 were calculated using a quasi-static approximation for the exponential term. The result for the x-component of $\vec{H}^d$ (coplanar loops) is

$$H_x^d = \frac{m_x e^{-jkr}}{4\pi}\left[\frac{3(y^2 + z^2)}{(x^2 + y^2 + z^2)^{5/2}}\right] \qquad \text{[Eq 17]}$$

The result for the z-component (coaxial loops) is

$$H_z^d = \frac{m_x e^{-jkr}}{4\pi}\left[\frac{3\,x\,z}{(x^2 + y^2 + z^2)^{5/2}}\right] \qquad \text{[Eq 18]}$$

To calculate these magnetic field components, Eqs 17 and 18 were integrated over the slits after making the substitutions

$$x = x - x'$$

$$y = y - y'$$

$$z = z - z' \qquad \text{[Eq 19]}$$

where the primed coordinate system has its origin in the aperture and the unprimed system is centered at the observation point (the center of the receiving loop). These integrals were carried out over the primed variables via standard numerical techniques in two FORTRAN programs SLITCP (SLIT CoPlanar) and SLITCA (SLIT CoAxial). (Listings of SLITCP and SLITCA appear in Appendix B.) Reference field strengths were calculated at the center of the receiving loops via the standard field equations for an elementary loop. Shielding effectiveness was then calculated for the coplanar orientation as:

$$SE = 20 \log \frac{H_x^{Ref}}{H_x^d} \qquad \text{[Eq 20]}$$

and for the coaxial orientation as:

$$SE = 20 \log \frac{H_z^{Ref}}{H_z^d} \qquad \text{[Eq 21]}$$

Figures 6 and 7 present the results of the program SLITCP and the experimental measurements taken for the coplanar loops. Also included are the predictions of the transmission line theory approach from Figures 3 and 4. The agreement between the Dipole-Moment Approximation technique and the experimental measurements approaches 1 dB for the smaller slot and represents about a 17-dB improvement in accuracy over the transmission line theory approach.

Figures 8 and 9 given the measurements taken with loop antennas in the coaxial orientation and the predictions of the computer program SLITCA. For this orientation, the agreement between experimental results and the Dipole-Moment Approximation prediction again improves slightly as the slot size decreases. For the smaller slot, the average of the experimental results is 46 dB, while SLITCA predicts 42.6 dB of shielding over the frequency band.

In summary, the results of these experimental measurements showed that extension of the Shelkunoff transmission line theory of shielding to slotted shields yielded inaccurate results, especially for coplanar test loops. A more promising technique is the Dipole-Moment Approximation, which yielded accurate predictions for electrically small slots. Butler[11] has extended the Dipole-Moment Approximation and related techniques to deal with more complicated, practical openings, such as hatch apertures.

[11] C. M. Butler, "Dipole Moment Approximation and Polarizabilities," Section 2.1.3.2 in *EMP Interaction Principles, Techniques, and Reference Data*, EMP Interaction 2-1, AFWL-TR-80-402 (Air Force Weapons Lab, Air Force Systems Command, December 1980).

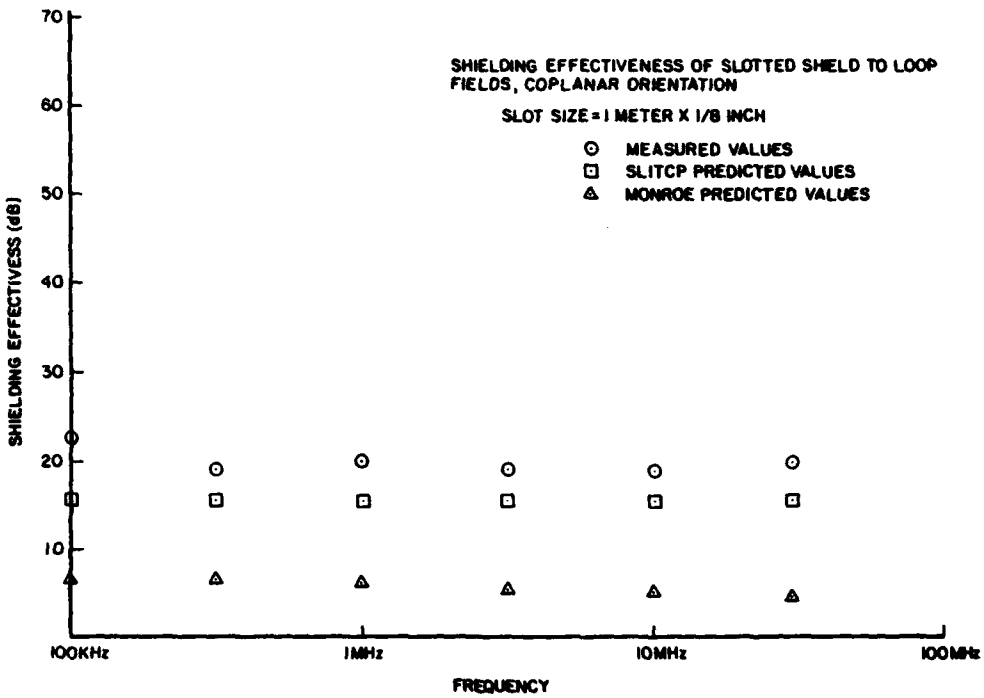

Figure 6. Shielding effectiveness of slotted shield to loop fields, coplanar orientation. Slot size = 1 m X 1/8 in.

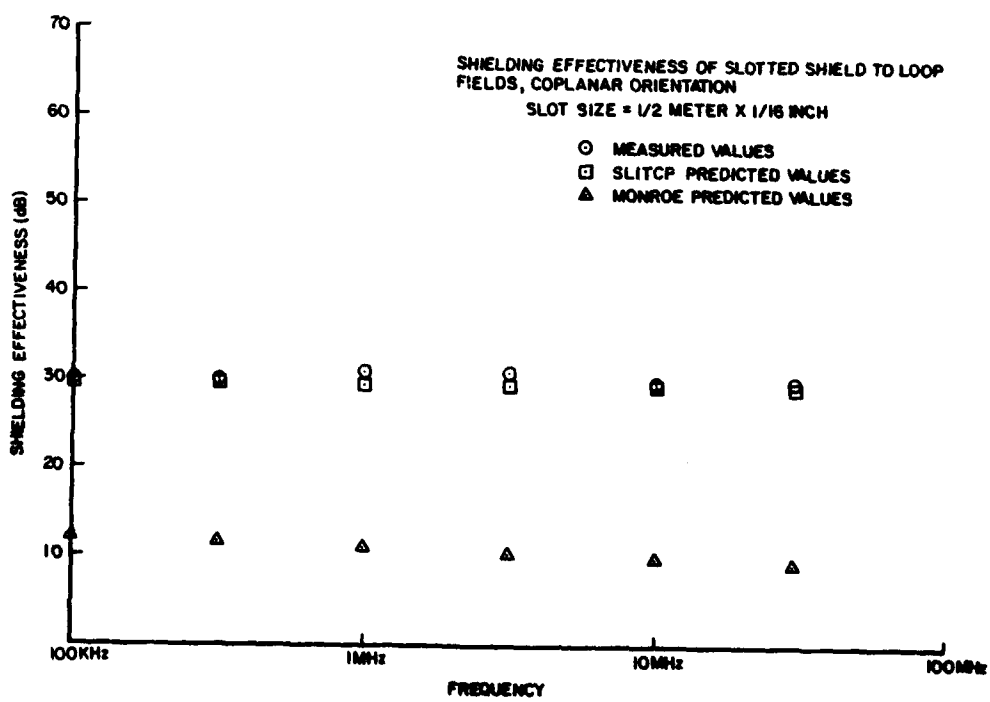

Figure 7. Shielding effectiveness of slotted shield to loop fields, coplanar orientation. Slot size = 1/2 m X 1/16 in.

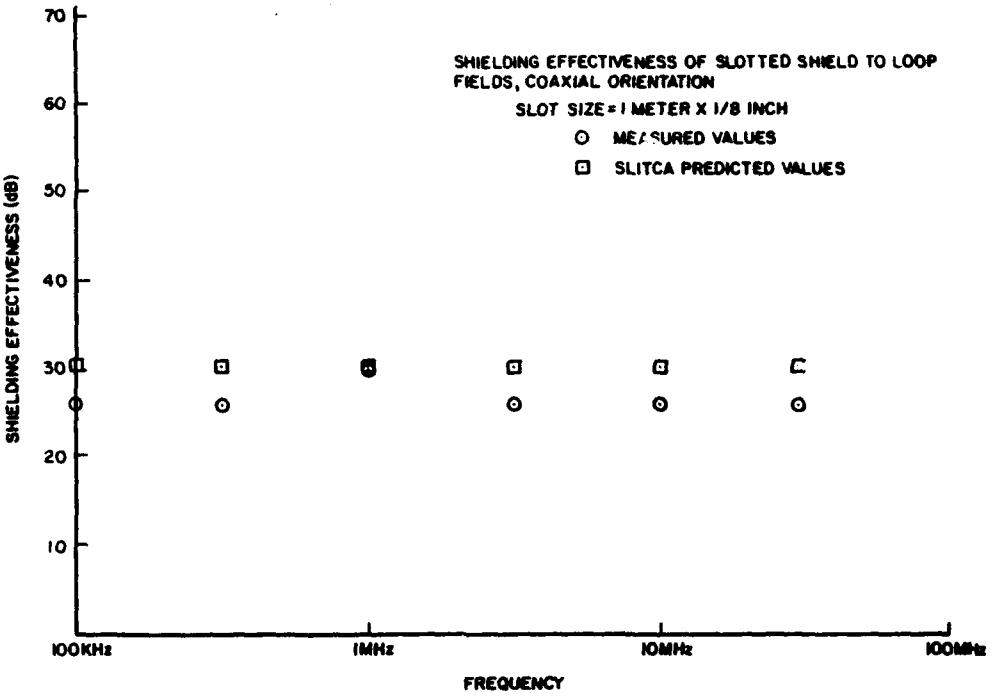

Figure 8. Shielding effectiveness of slotted shield to loop fields, coaxial orientation. Slot size = 1 m X 1/8 in.

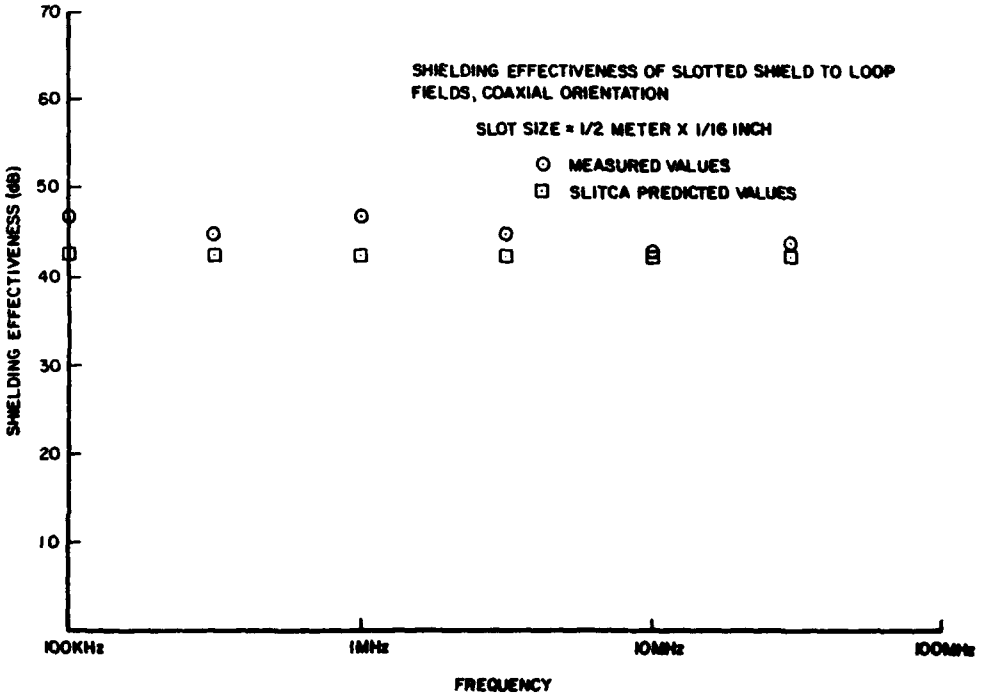

Figure 9. Shielding effectiveness of slotted shield to loop fields, coaxial orientation. Slot size = 1/2 m X 1/16 in.

4 SHIELDING EFFECTIVENESS OF MULTIPLE-LAYER SHIELDS

The construction of the Ground Launch Cruise Missile shelter outer casing is a composite of plane sheets of laminated conductor and structural materials. The conductor sheets provide electromagnetic shielding while at least one filler layer is used to increase rigidity. There is a lack of research literature about the development of the capability to calculate the shielding effectiveness of plane-laminated materials. This chapter describes a technique developed during this investigation for calculating the shielding effectiveness of multiple-layer shields for loop antennas in the coaxial configuration. This technique is based on the plane-wave spectrum approach. Also included is a discussion of the computer programming of these relations, as well as experimental assessment of their validity and accuracy.

Tyras[12] gives the transfer function for plane wave propagation through multiple planar layers of arbitrary material. Figure 10 shows the geometry and notation used. The transfer function of the multiple plane layers is given by:

$$T = \frac{2 Z_{m+1}}{S_1 + Z_1} \prod_{p=2}^{m} \frac{S_{p-1}}{S_p \cos \Psi_p - i Z_p \sin \Psi_p} \qquad \text{[Eq 22]}$$

$$S_{p-1} = Z_p \left(\frac{S_p - i Z_p \tan \Psi_p}{Z_p - i S_p \tan \Psi_p} \right) \qquad \text{[Eq 23]}$$

$$\Psi_p = k_{pz} d_p \qquad \text{[Eq 24]}$$

where:

p = material layer: p=1, 2..., m+1
p=1 is the incident half-space
p=m+1 is the transmission half-space

m+1 = total number of layers (including half-spaces)

m-1 = total number of shielding and structural layers

d_p = depth of a shielding or structural layer

k_{pz} = complex propagation constant in the z direction for layer p

Z_p = intrinsic impedance of a layer

S_p = input impedance at p^{th} interface

Eq 23 is a recursive relation for calculating S_p. The calculation begins by setting the input impedance at the last interface equal to the intrinsic impedance of the transmission half-space:

$$S_m = Z_{m+1} \qquad \text{[Eq 25]}$$

Computational effort is reduced by combining Eqs 22 and 23 to obtain:

$$T = \frac{2}{1 + \zeta_1} \prod_{p=2}^{m} \frac{1}{\cos \Psi_p (1 + i \zeta_p \tan \Psi_p)} \qquad \text{[Eq 26]}$$

in which

$$\zeta_p = \frac{S_p}{Z_p} \qquad \text{[Eq 27]}$$

The values for ζ_p are obtained by dividing Eq 23 through by Z_{p-1} and rearranging to obtain:

$$\zeta_{p-1} = \frac{S_{p-1}}{Z_{p-1}} = \frac{Z_p}{Z_{p-1}} \frac{\zeta_p - i \tan \Psi_p}{1 - i \zeta_p \tan \Psi_p} \qquad \text{[Eq 28]}$$

[12] George Tyras, *Radiation and Propagation of Electromagnetic Waves* (Academic Press, 1969), pp 40–43.

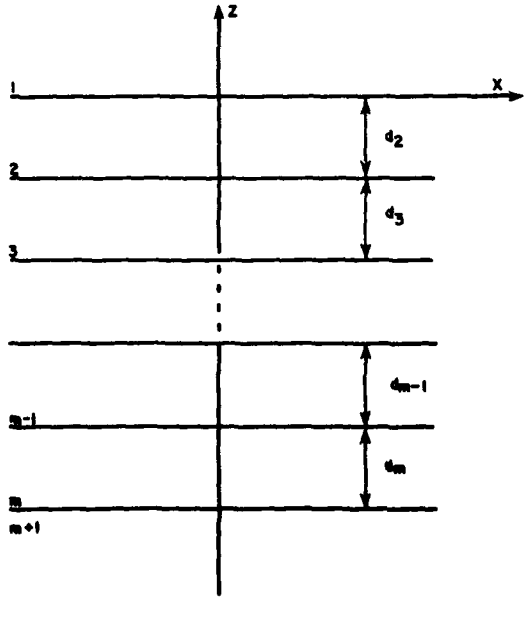

Figure 10. Geometry and notation for multiple-layer planar shield.

in which the recursion is now started by setting

$$\zeta_{m+1} = \frac{S_{m+1}}{Z_{m+1}} = 1 \qquad \text{[Eq 29]}$$

The transfer function given in Eq 26 applies to plane waves incident upon a multiple-layer medium. It is extendable to the case of the nonplanar radiation of a loop antenna if the fields of the loop antenna are expressed as an angular spectrum of plane waves.

Moser[13] provides the derivation of the shielding effectiveness of a single-layer, planar shield for loop antennas in the coaxial configuration. This work was later pursued by Bannister.[14] The equation for shielding effectiveness, SE, is:

$$SE \approx -20 \log \left[\frac{4\mu_r}{a} (a^2 + z^2)^{3/2} \cdot \int_0^\infty \frac{C\lambda^2 \tau}{\tau_o^2} J_1(\lambda a) \exp\{-\tau_o z - t(\tau - \tau_o)\} d\lambda \right] \qquad \text{[Eq 30]}$$

where:

$C = [(\tau/\tau_o + \mu_r)^2 - (\tau/\tau_o - \mu_r)^2 e^{-2t\tau}]^{-1}$

$\tau = (\lambda^2 + \gamma^2)^{1/2}$

$\tau_o = (\lambda^2 + \gamma_o^2)^{1/2}$

$\gamma_o = i\, 2\pi/\lambda_{air}$, the free space propagation constant

$\approx (iw\mu_o\mu_r\sigma)^{1/2}$, the propagation constant in the shield

$\tau_r = |\alpha|/\{\overline{2} = (w\mu_o\mu_r\sigma/2)^{1/2} = 1/\delta$

$\delta = (2/w\mu_o\mu_r\sigma)^{1/2}$, the skin depth in the shield

μ_r = relative permeability of the shield

t = shield thickness

$\mu_o = 4\pi \times 10^{-7}$, permeability of free space

$\sigma = (5.8 \times 10^7)\sigma_r$, conductivity of the shield

σ_r = relative conductivity of the shield with respect to copper

a = radius of the loop antenna

$z = r_1 + r_2$, the center-to-center separation of the transmitting and receiving loop antenna

$J_1(\lambda a)$ = the Bessel function of order one and argument λa.

The Bessel function term corresponds to a plane wave spectrum description of the fields due to the loop source.

Eq 3 may be expressed in terms of the transfer function for the shield, $T(\lambda)$:

$$SE \approx -20 \log \frac{(a^2 + z^2)^{3/2}}{a} \int_0^\infty \frac{\lambda^2}{\tau_o} T(\lambda) J_1(\lambda a) \exp\{-\tau_o(z-t)\} d\lambda \qquad \text{[Eq 31]}$$

where:

$$T(\lambda) = \frac{4\mu_r C\tau}{\tau_o} e^{-\tau t} \qquad \text{[Eq 32]}$$

After some algebraic operations, it may be shown that the multiple-layer transfer function given by Eq 26 reduces to Eq 32 for the case m+1 = three total layers. This is the case for a single plane shield, with air as the half-space layers on each side. Eq 31 is also the generalized version of the expression for the shielding effectiveness of a single layer shield; this equation is useful for computing the shielding effectiveness of the multiple layer case once the transfer function $T(\lambda)$ is calculated according to Eq 26.

Before Eq 26 can be used in Eq 31, one must convert the notation for Tyras' propagation constant to that used by Moser and Bannister. Tyras defines the square of the propagation constant as:

$$k^2 = \omega^2\mu\epsilon + i\sigma\omega\mu \qquad \text{[Eq 33]}$$

while Bannister uses the definition

$$\gamma^2 = -\omega^2\mu\epsilon + j\sigma\omega\mu \qquad \text{[Eq 34]}$$

These two notations can be related by letting

[13] J. R. Moser, "Low-Frequency Shielding of a Circular Loop Electromagnetic Field Source," *IEEE Transactions on Electromagnetic Compatibility*, Vol EMC-9, No. 1 (March 1969).

[14] P. R. Bannister, "Further Notes for Predicting Shielding Effectiveness for the Plane Shield Case," *IEEE Transactions on Electromagnetic Compatibility*, Vol EMC-11, No. 2 (May 1969).

$$-\gamma^2 \approx -k^2 \qquad \text{[Eq 35]}$$

$$j = -i \qquad \text{[Eq 36]}$$

The change indicated in Eq 36 is dictated by the fact that the time convention used in this work is $e^{j\omega t}$, as opposed to $e^{-i\omega t}$ as used by Tyras.

Now the multiple-layer transfer function given by Eq 26 must be expressed in terms of the angular frequency integration constant, λ, used in Eq 31. First, Ψ_p in Eq 24 is written as a function of τ_p.

$$\Psi_p = k_{pz} d_p = -i\,\tau_p d_p = j\,\tau_p d_p \qquad \text{[Eq 37]}$$

Next, τ_p is written as a function of λ:

$$\tau_p = \sqrt{\lambda^2 + \gamma^2} \qquad \text{[Eq 38]}$$

Putting Eqs 37 and 38 into Eq 26 and converting to hyperbolic functions yields:

$$T(\lambda) = \frac{2}{1+\zeta_1} \prod_{p=2}^{m} \frac{1}{\cosh(\tau_p d_p)[1 + \zeta_p \tanh(\tau_p d_p)]} \qquad \text{[Eq 39]}$$

$$\zeta_{p-1} = \frac{\mu_{rp}\,\tau_{p-1}}{\mu_{r(p-1)}\,\tau_p} \frac{\zeta_p + \tanh(\tau_p d_p)}{1 + \zeta_p \tanh(\tau_p d_p)} \qquad \text{[Eq 40]}$$

$$\zeta_{m+1} = 1 \qquad \text{[Eq 41]}$$

where

$$\frac{Z_p}{Z_{p-1}} = \frac{\mu_{rp}\,\tau_{p-1}}{\mu_{r(p-1)}\,\tau_p} \qquad \text{[Eq 42]}$$

has been substituted into Eq 40. This is the form of the multiple-layer transfer function used in the integral expression (Eq 31).

The above equations were programmed on a CDC 7600 computer via the FORTRAN program MULSH (MULtiple SHields)(see Appendix B). Using $d\lambda = 0.10$, the integral expression in Eq 31 converged to a relative error of 10^{-6} within 1000 steps. (This control parameter may have to be changed if problem dimensions differ appreciably from those studied in this work.) MULSH allows the user to specify a shield design having one to five total shielding and/or structural layers of any thickness and material. (It should be noted that MULSH assumes an infinitely large shield.)

To assess the validity and accuracy of MULSH, shielding effectiveness measurements were taken in the laboratory on panels composed of two 1-mil-thick copper sheets separated by either a 1/8-in. or 1/2-in. thickness of masonite (nonconductive material for structural support). These panels were mounted over the 2- x 4-ft aperture in a shielded room. LP-105 loop antennas (12-in. diameter) were used for measurements greater than 100 kHz; 22 1/2-in. diameter loops made at CERL were used for measurements at and below 100 kHz.

Initial comparisons between experimental shielding effectiveness measurements and MULSH predictions indicated that MULSH consistently underestimated shielding effectiveness in the 10-kHz to 1-MHz range by about 10 dB. However, this was not surprising, since MULSH models an infinitely large (height and width) double-copper-foil panel, whereas the experimental setup consisted essentially of a 2- x 4-ft, double-foil aperture in an otherwise opaque screen.

To evaluate MULSH more completely, another program was developed to account for the geometry of the aperture in the experimental setup. This program, called APRAD (APerture RADiation), calculates the radiation of fields of a loop antenna (coaxial configuration) through an aperture containing a single thin conducting sheet in an otherwise opaque screen. APRAD is listed in Appendix B. Although APRAD was developed for this special case, the theoretical techniques used in its derivation can be extended to the general problem of calculating radiation through apertures.

The formulas used to develop APRAD are based on the application of Huygen's principle.[15] The fields on the transmission side of the foil aperture can be expressed in terms of the tangential electric field impressed on the incidence side of the foil by the transmitting loop antenna. Since the receiving loop responds to the magnetic field normal to the plane of the loop, only the magnetic field is calculated on the transmission side of the screen. This is given by:

$$H(\vec{r}) = (j\omega\epsilon_o)^{-1} (\vec{\nabla} \times \vec{\nabla} \times \vec{F}(\vec{r})) \qquad \text{[Eq 43]}$$

where:

$$\vec{F}(\vec{r}) = \frac{1}{4\pi} \iint_{Ap} \frac{\vec{M}(\vec{r}')}{|\vec{r} - \vec{r}'|} e^{-jk|\vec{r} - \vec{r}'|}\, dr'$$

[15] R. F. Harrington, *Time-Harmonic Electromagnetic Fields* (McGraw-Hill Book Company, Inc., 1961), p 110.

and

$\vec{M}(\vec{r}') = T(\lambda)(2\vec{E}_{tan} \times \hat{n})$; magnetic current in foil

$\omega = 2\pi f$; f = frequency in Hz

$k = 2\pi/\lambda$

$\epsilon_o = 8.854 \times 10^{-12}$ F/m

$\vec{r}' = (x'\hat{x} + y'\hat{y})$: vector from origin in plane of aperture to a point in the plane of the aperture

$\vec{r} = (x\,\hat{x} + y\,\hat{y} + R_{rec}\,\hat{z})$: vector from origin in plane of aperture to a point in the plane of the receiving antenna located R_{rec} meters from aperture

$T(\lambda)$ = transfer function of sheet as calculated in Eq 39

$\lambda = \sqrt{u^2 + v^2}$: angular frequency variable

$u = (2\pi/\lambda)\sin\theta\cos\Phi$

$v = (2\pi/\lambda)\sin\theta\sin\Phi$

θ, Φ = angles of a spherical coordinate system with origin at the center of the transmitting loop and Z axis coaxial with the transmitting and receiving loops.

As outlined by the above equations, the approach taken in APRAD is as follows. First, the tangential electric field is calculated on the incidence side of the aperture from the standard equations for the fields produced by a small (compared to wavelength) loop. Then the electric field is passed through the foil using the transmission coefficient of Eq 39 for a single layer; the coefficient is evaluated at values of λ corresponding to angles that the aperture intercepts. In the case of the 2- x 4-ft aperture, the electric field is evaluated on a 5 x 9 sample point grid centered on the aperture. The transfer function is the same one used in MULSH; however, in APRAD, it is evaluated only for angular frequencies corresponding to angles intercepted by the aperture. In MULSH, an infinite sheet is assumed. Thus, the transfer function in MULSH appears as an integral over λ, with an infinite limit of integration.

After the electric field is passed through the foil, a magnetic current flowing in the foil is expressed as a cross product of the reduced electric field and the normal vector to the foil surface. Then an electric vector potential, F (dual of a magnetic vector potential), is expressed as an integral (sum) over the sample points of the magnetic current in the foil. From the electric vector potential, the magnetic field in the plane of the receiving loop antenna is calculated via a double curl operation.

In performing the derivatives for the double curl, a quasi-static approximation was made by assuming that the exponential term within the integral for F was constant. This was justified, since $|\vec{r} - \vec{r}'|$ varies by less than a factor of 2 over the aperture, and k has a maximum value of .021 in the frequency band of interest. The normal component of the magnetic field is calculated within the receiving loop at 7 points and integrated to give the received signal strength. To calculate shielding effectiveness, a reference response is calculated for the loop antenna (separated by an appropriate distance of free space) directly from the field equations for a small loop. The normal component of the magnetic field is again calculated at 7 points in the receiving loop and integrated.

To correct the MULSH predictions for the experimental setup, APRAD and MULSH are both run for a single 1-mil copper sheet. The difference between the shielding effectiveness predicted by the two programs is termed the "Blockage Factor" and accounts for the opaque part of the shielded room wall. Computational results have shown that the Blockage Factor for this experimental setup is about 10 dB, thus accounting for MULSH's 10-dB underestimate of shielding effectiveness.

Figure 11 shows the predicted values of shielding effectiveness produced by MULSH and APRAD for a single, 1-mil-thick, copper sheet. Also shown are experimental measurements for the single copper sheet and the difference between the predictions of MULSH and APRAD (the Blockage Factor). Note that the APRAD predictions show reasonable correlation with the experimental measurements except at 10 MHz, where the experimental accuracy is highly suspect.

Figure 12 shows the MULSH predictions as corrected by addition of the Blockage Factor for the two double-copper foil shields. Notice the increase in shielding effectiveness as the separation between the sheets is increased from 1/8-in. to 1/2 in. This can be explained by examining the behavior of S_1 (Eq 23), the input impedance at the first air-copper interface. As the separation between the copper sheets increases, S_1 decreases (numerical results from MULSH). Consequently, the

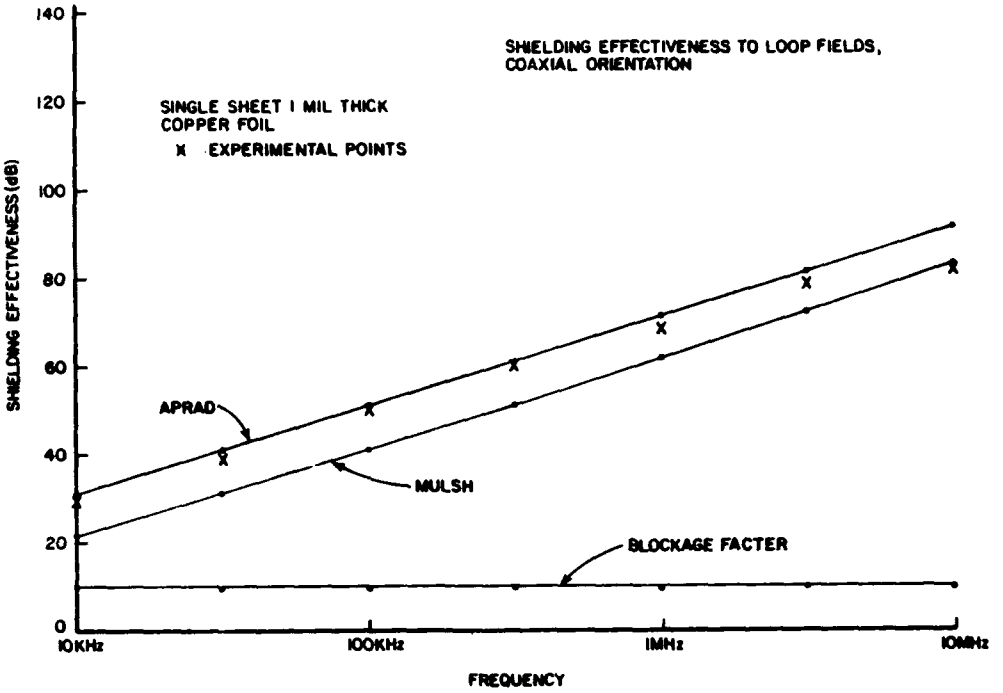

Figure 11. Shielding effectiveness of single copper sheet (1-mil-thick) to loop fields, coaxial orientation.

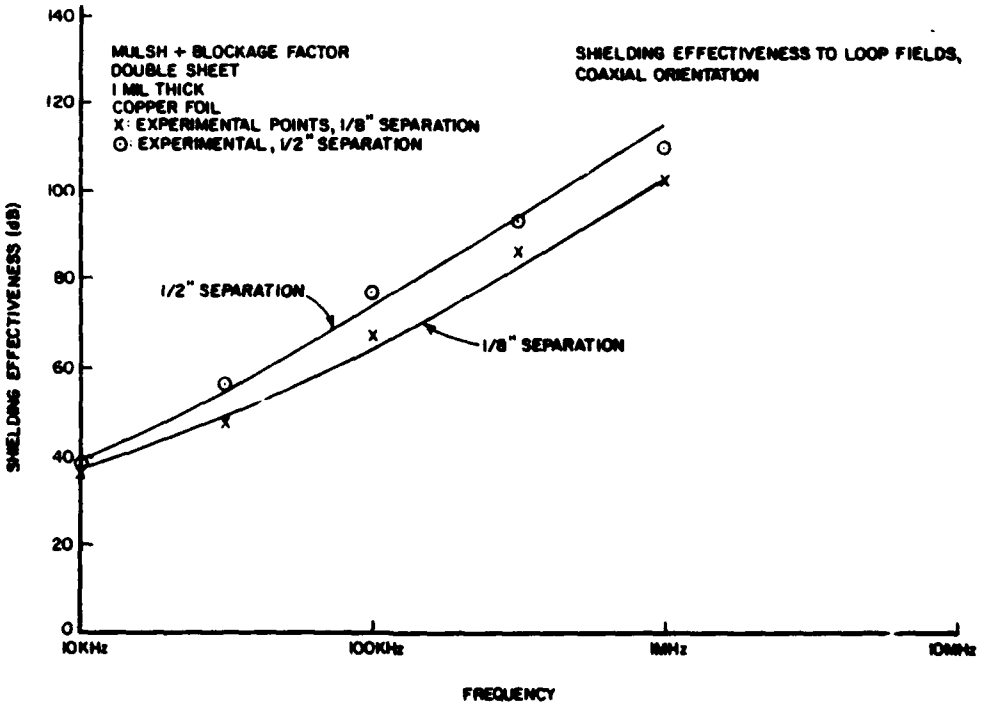

Figure 12. Shielding effectiveness of double copper shield to loop fields, coaxial orientation.

mismatch between the impedance of the multiple layer shield and the impedance of the incident wave is increased. This increases the reflection from the interface, thus increasing shielding effectiveness.

In summary, a plane wave spectrum approach was used to calculate the shielding effectiveness of a multiple layer shield to the fields of a loop antenna positioned in the coaxial test configuration. To model the aperture of the experimental setup more accurately, Huygen's principle was used to express the fields on the transmission side of the aperture (containing a single, thin-layer shield) in terms of the fields incident on the aperture. When these two approaches are combined (APRAD and MULSH, and the Blockage Factor), the results are in good agreement with the experimental results. Appendix A presents an extension of the plane wave spectrum approach to calculating the shielding of a multiple-layer medium to arbitrary incident radiation.

5 CAVITY RESONANCE EFFECTS

A screen's EMP shielding effectiveness can often be estimated from its CW performance. However, for a cavity-type structure (e.g., an enclosed shelter), behavior near its interior resonances cannot be directly extrapolated to estimate the strength of EMP penetration into the shelter. The effect of resonance on the CW field penetration into the interior of cavity-type configurations has been investigated and documented by Mittra[16] and by Yung.[17]

Figure 13 shows that the field at the center of an infinitely long cylinder can become quite large near its interior resonance. Figure 14, which shows the induced current in a wire located inside a cylindrical cavity with an aperture, also exhibits a similar phenomenon. However, to compute the transient response of these structures, one must first multiply the frequency response of the structure and the spectrum of the incident EMP field. Butler[18] provides an example of such a computation. Figure 15 shows the frequency response of a screen with an aperture; Figure 16 exhibits the transient response of the same response for an incident EMP whose waveform is shown in the inset of the same figure. As shown, the primary effect of the resonance is to introduce ringing in the transient response; the frequency of the ringing is determined by the resonant frequency of the cavity, while the decay envelope is determined by the width of the resonance. The energy deposited by the incident pulse within the resonant bandwidth of the cavity primarily determines the peak of the ringing waveform. Consequently, the height of this peak is not enhanced nearly as dramatically as the resonance peak of the frequency response curve; this is because the incident EMP pulse seldom contains much energy in the resonance band of the cavity.

The worst case energy coupling into a tactical shelter at a cavity resonance frequency can be roughly calculated as follows. For typical shelter dimensions, the lowest cavity resonance will be around 100 MHz. Figure 17 illustrates the normalized power spectrum for an EMP; the energy content at 100 MHz is 60 dB below the peak value of .075 V/m-Hz at 700 kHz. Thus, the power density incident on the shelter in a 1-Hz band width is given by:

$$P_d = \frac{1}{2}\frac{(.075 \times 10^{-3})^2}{377}$$

$$= 7.46 \times 10^{-12}\ \omega/m^2 - Hz \qquad [Eq\ 44]$$

If the EMP is incident on a shelter with a wall of, say, 3 x 7 m, then, with no shielding, the power coupled into the shelter would be:

$$P = (21\ m^2)(7.46 \times 10^{-12}\ \omega/m^2 - Hz)$$

$$= 1.57 \times 10^{-10}\ \omega/Hz \qquad [Eq\ 45]$$

for a 1-Hz band width. Even for a 1-kHz band width, this is still only .157 μW of power in the resonant band, without considering the shielding. Since a high-performance shelter will probably have at least 100 dB of shielding to a plane wave at 100 MHz, cavity resonances of tactical shelters are not expected to be stimulated by EMPs.

[16] R. Mittra, "Cavity Excitation via Apertures," *EMP Interaction: Principles, Techniques and Reference Data*, Ch. 2.3.2.1, K. S. H. Lee, ed. (Air Force Systems Command, December 1980), pp 522-523.

[17] E. K. Yung, S. W. Lee, and R. Mittra, "Penetration of an EM Wave into a Cylindrical Cavity and the Current Induced on a Wire Inside," *AEU*, Band 33, Heft 4 (1979), pp 149-156.

[18] C. M. Butler, Y. Rahmat-Samii, and R. Mittra, "Electromagnetic Penetration Through Apertures in Conducting Surfaces," *IEEE Trans. on Antennas and Propagation*, Vol AP-26, No. 1 (January 1978), pp 82-93.

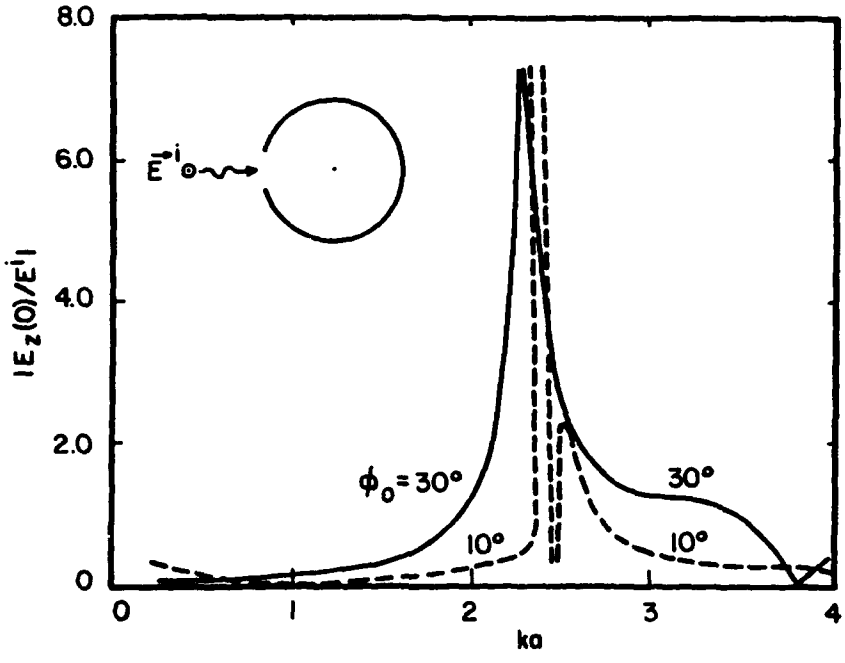

Figure 13. Variation of interior field along $\phi = 0°$, with ka as parameter for field at the center of the cavity versus ka for $\phi_0 = 10°$ and 30°.

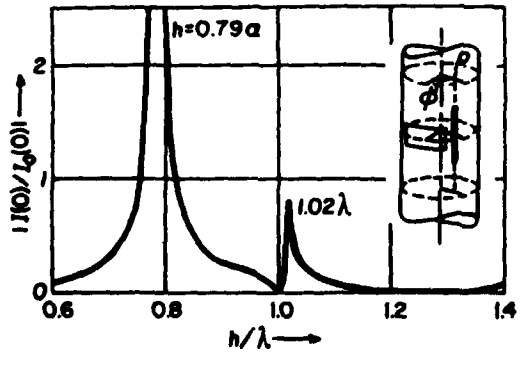

Figure 14. Induced current at the center of the wire inside the cavity as a function of cavity length 2h. The geometrical parameters are: a = 0.5 λ, c = 0.3 λ, d = 0.015 λ, a_w = 0.001 λ, h_w = 0.2 λ, e/a = 0.1.

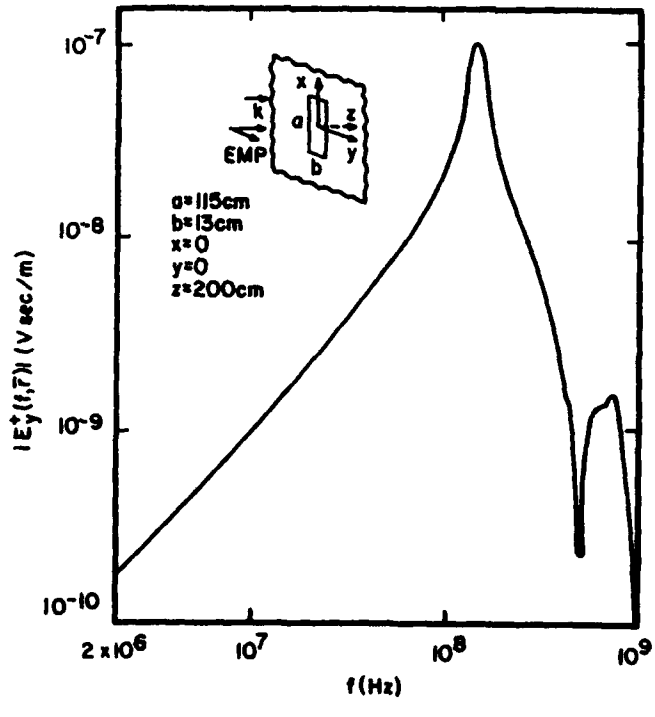

Figure 15. Frequency domain behavior of $|E_y^s(f, \underline{r})|$ sampled at a point 2 m behind the aperture.

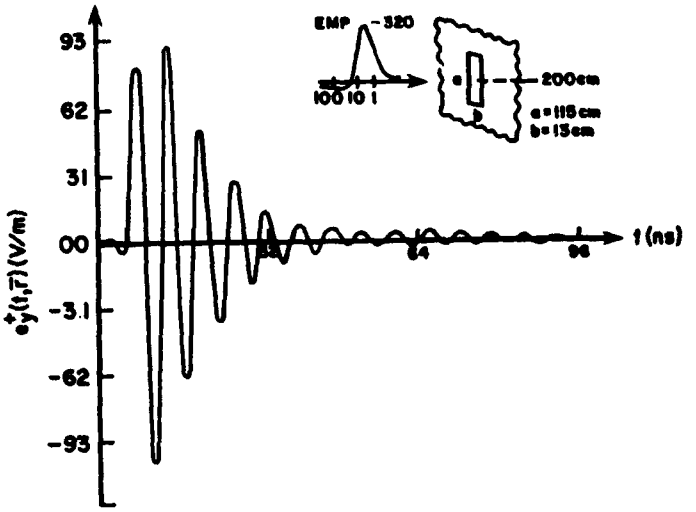

Figure 16. Time domain behavior of the $e_y^+(t, \underline{r})$ field sampled at a point 2 m behind a single aperture.

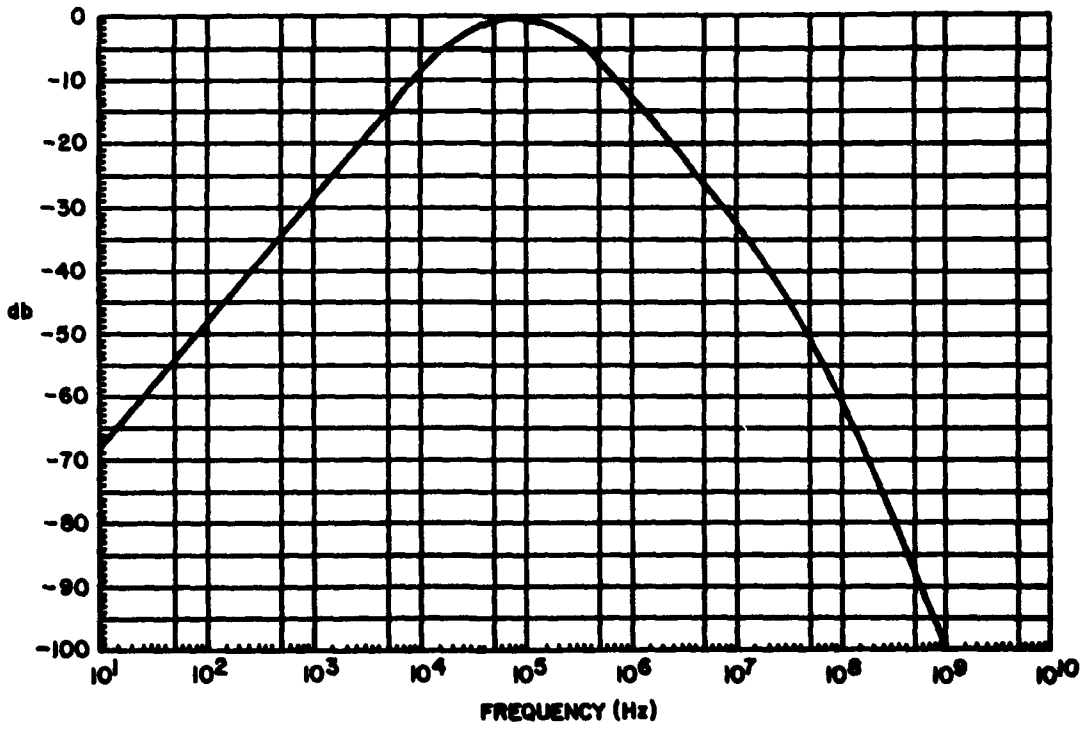

Figure 17. Normalized EMP power spectrum. (From *EMP Protection for Emergency Operating Centers* TR-61A, [Department of Defense, July 1972]).

6 SHELTER TEST PROCEDURES RECOMMENDATIONS

Discussion

As stated in Chapters 1 and 2, when it is not possible or practical to use an EMP simulator to evaluate shielded structures, rooms, zones, etc., it is customary to substitute test methods described in MIL-STD-285,[19] IEEE 299,[20] or NSA 65-6.[21]. These and similar procedures require testing at discrete CW frequencies using small antennas such as loops, dipoles, monopoles and horns. Problems or shortcomings of this type of testing include the following:

1. Using loops or dipoles for CW testing involves testing with either low (loop) or high (dipole or monopole) wave impedance fields through most of the frequency range of interest. Monroe[22] and Villaseca[23] have shown that shielding effectiveness values resulting from these measurements can be related to shielding effectiveness for plane waves where the wave impedance is 377 ohms. These conversions, however, have not gained wide acceptance.

2. The EMP transient has spectral energy distributed over a relatively broad frequency range. For complete testing, a continuous frequency scan should be taken of the entire EMP frequency range. Experience has shown, however, that the shielding effectiveness of shielded structures such as rooms and shelters tends to follow a relatively smooth curve at frequencies below 20 MHz. Therefore, the curve up to 20 MHz can be approximated by obtaining a few measurements at discrete frequencies. However, at frequencies above 20 MHz, problems in taking the CW shielding measurements begin to occur. These problems are related to reflections and standing waves within the shielded volume being tested, which cause large variations and lack of repeatability of test data. The reflections are further complicated by the effects of test personnel movements and the changes in measured test data caused by small changes in transmitting antenna orientation relative to a defect. Thus, trying to obtain a good, average CW shielding effectiveness value above 20 MHz is time-consuming and requires skilled and persistent test operators. At best, the data taken above 20 MHz will have doubtful repeatability within 5 dB and even worse repeatability as frequency is increased.

3. Another problem in CW testing is the inability to account for the effect of numerous cavity resonances. These resonances are defined by the mathematical expression:

$$f_r = 150\sqrt{\left(\frac{m}{a}\right)^2+\left(\frac{m}{b}\right)^2+\left(\frac{p}{c}\right)^2}, \text{MHz} \quad \text{[Eq 46]}$$

where:

a, b, and c are interior dimensions of the enclosure in meters.

m, n, and p are integers, only one of which may be zero at a time.

For typical room-sized enclosures, the lowest resonance is near 100 MHz, but resonances are lower for larger enclosures. The problems caused by the resonances are: (a) apparent shielding effectiveness at a specific resonance may be much lower than actual shielding effectiveness at frequencies away from resonances, and (b) it is difficult to use CW test techniques for all resonances without a sweeping/tracking transmitter/receiver system. In an EMP simulator, the transient pulse has spectral components which may excite all enclosure resonances simultaneously; thus, the combined resonance effects may be measured for each simulator pulse. However, simulator tests cannot generally provide the absolute worst-case resonance effects either, because the amount of excitation of wave guide modes within the enclosure is uncertain.

Summary of the State of the Art in CW Testing

Consideration of the current state of the art in CW shielding effectiveness testing should account for (1)

[19] *Military Standard Attenuation Measurements for Enclosures, Electromagnetic Shielding for Electronic Test Purposes, Method of,* MIL-STD-285 (Department of Defense, 25 June 1956).

[20] *Proposed IEEE Recommended Practice for Measurement of Shielding Effectiveness of High-Performance Shielding Enclosures,* IEEE 299 (Institute of Electrical and Electronics Engineers [IEEE], June 1969).

[21] P. R. Trybus, *National Security Agency Specification for R.F. Shielded Enclosures for Communications Equipment: General Specification,* NSA 65-6 (National Security Agency, 30 October 1964).

[22] R. L. Monroe, *EMP Shielding Effectiveness and MIL-STD-285,* HDL-TR-1636/AD771997 (Harry Diamond Laboratories, U.S. Army Materiel Command, July 1973).

[23] E. Villaseca, C. Davis, W. Blackwood, and W. Getson, *An Investigation of the Validity of Applying MIL-STD-285 to EMP Shielding Effectiveness,* ADA051889, prepared by Harris Corp. Electronics System Division (Defense Nuclear Agency, 15 April 1977).

standard test specifications and recent work to upgrade them, (2) test methods regarded within the industry as "acceptable," and (3) recent work to develop new approaches. These are discussed below.

Standard Test Specifications

Currently, there are two standard test specifications (MIL-STD-285 and NSA 65-6) and one proposed standard (IEEE 299). No modifications to these standards have been published since their initial printings. The former U.S. Army Electronics Command did some preliminary work in the mid-1970s to revise MIL-STD-285, but it was not completed. Other efforts to revise the IEEE 299 standard are as yet unpublished.[24] A preliminary draft of these revisions has noted that no significant changes to the testing methods are recommended. There have been no known attempts to revise NSA 65-6.

Recently, the Mission Research Corporation prepared a "Specification for EMP Attenuating Prototype Air Force Tactical Shelter"[25] for the Air Force Weapons Laboratory (AFWL). This specification, which includes a section on EMP testing, states that three separate tests should be done on the shelter: (1) extended MIL-STD-285 testing, (2) EMP simulation tests, and (3) EMP hardness maintenance checks. The extended MIL-STD-285 tests differ from MIL-STD-285 only in that more frequencies are specified in H-field, E-field, and plane wave testing, and more test point locations are specified. The EMP simulation tests require a EMP simulator. The EMP hardness maintenance checks are done with a radio frequency (RF) seam sniffer.

Specifications for CW testing of SAFEGUARD facilities have been published by the Army.[26] These methods use the same principles set forth in MIL-STD-285 with some slight modifications.

Test Methods Used by Industry

Shielded room manufacturers have used some significantly abbreviated test methods for EMI shielding evaluations. They feel that these abbreviated procedures indicate EMP shielding adequately. The procedures use a seam leak detector to locate leaks and establish relative signal leakage magnitudes. The seam leak detection method uses CW current injection at about 100 kHz; the current injection points are located on diagonally opposite corners. Generally, one set of measurements is taken with injection on one set of corners, but repeated using another set. Worst readings are taken as representative.

Typically, shelter manufacturers closely follow the procedures of MIL-STD-285 to measure EMI/RFI shielding effectiveness. However, they use the minimum number of antenna test positions allowed by MIL-STD-285 around the shelter.

CW testing has been used to verify EMP hardness of large facilities, such as Minuteman Missile structures, the SAFEGUARD ABM structures, the Systems Technology Test Facility (STTF) on Meck Island, and numerous secure communications facilities.

Development of New CW Test Methods

Two programs are considering CW testing for EMP hardness evaluation. AFWL is developing specialized antennas called plane wave launchers. AFWL has already developed a test concept known as the PARTES concept, in which a planar array of small antenna elements (loop or monopole) generates a propagating wave with a nearly planar wavefront. These antenna arrays can be used with CW excitation and will allow CW testing. This can provide actual plane wave shielding effectiveness data without the uncertainty caused by a nonplanar (spherical) wavefront, as generated by loop and dipole antennas. However, the problem of accounting for resonances is still not solved by the plane wave test approach.

In another program, the Defense Nuclear Agency (DNA) is investigating the use of a sophisticated transmitter and receiver system which has a very high measurement range and the capability to obtain swept frequency measurements between 10 kHz and 100 MHz. This system can measure shielding effectiveness magnitudes according to MIL-STD-285 specifications and also measure the phase function over the entire frequency range in discrete frequency steps smaller than 1 Hz. Thus, it is possible to obtain magnitude and phase curves for CW shielding effectiveness over the frequency range containing more than 99.9 percent of the energy of a typical high-altitude EMP (HEMP) transient. Fourier analysis can be used to predict the

[24] *Proposed Revision of IEEE Recommended Practice for Measurement of Shielding Effectiveness of High Performance Shielding Enclosures* (Draft) (IEEE).

[25] A. G. Finei, H. M. Fowles, P. R. Trybus, *Ground Based C³ Facilities Hardening and Validation*, GBC³-3-MRC-064 (Mission Research Corporation, November 1980).

[26] H. E. Atkins, R. E. Evans, B. J. Gay, H. L. Holt, and A. R. Wright, *Safeguard Tactical Ground Facilities EMP/RFI Facilities Acceptance Construction/Installation Test Plan–Grand Forks*, prepared by the Boeing Company (U.S. Army Engineer Division, Huntsville, 6 January 1972).

EMP transient response from these curves, obviously excluding the effects of resonances and shielding effectiveness above 100 MHz.

In both of these programs, the systems are in the developmental phases and not ready for recommendation for tactical shelter maintenance testing. Reviews of the CW test methods are available in the literature.[27]

Summary

The following discussion summarizes the factors that led to test procedure recommendations discussed on pp 30 through 31.

The equipment needed for the new systems and concepts being studied by AFWL and DNA is not readily available for the widespread use required for periodic maintenance testing of tactical shelters. Furthermore, these systems will probably be too expensive for the intended applications and will require a greater amount of operator skill and/or data analysis than is desirable for maintenance testing.

In most applications for shelters of International Standards Organization (ISO) size or smaller, the effects of cavity resonances should not be significant, because more than 99.9 percent of the HEMP energy is below the lowest resonant frequency. (See Chapter 5.)

Experience has shown that at frequencies below 20 MHz, the shielding effectiveness versus frequency curve is relatively smooth and without discontinuities. Thus, it can be approximated by measurements at a few (three or four) appropriately spaced frequencies.

The shielding effectiveness measured for the CW nonplane wave can be related to the EMP plane wave shielding effectiveness by simple correction factors. (See Chapter 2.)

Using the appropriate correction factors, the approximated CW shielding response curve for a shielded volume, and Fourier analysis, the shielding for plane wave transients, such as those associated with HEMP, can be approximated.

It is unlikely that any radically new, low-cost methods for performing simple EMP tests on shielded structures will be developed without major effort.

In view of these points, CW testing continues to be the basic low-cost approach for assuring continuing EMP hardness of small shielded structures such as shelters. If EMP hardness of the shelter (with all internal equipment) is ascertained after it is manufactured and assembled, the CW test approach is especially useful for measuring any shielding deterioration. Thus, having concluded that CW testing will remain as a compromise method of testing EMP hardness, the test procedures to be used must be recommended. In a previous study, CERL investigated EMI test methods for tactical shelters.[28] The study concluded that IEEE 299 test methods are generally preferable to those outlined in MIL-STD-285. In addition, the following changes to IEEE 299 were recommended.

1. Where possible, use electrostatically shielded loops for the small loop magnetic field tests. If these loops give an inadequate dynamic measurement range, unshielded loops may be used. To increase measurement range, the unshielded loops should be used with multiple turns, resonance tuning, and impedance matching.

2. For general use, the coaxial loop antenna orientation is preferable to the coplanar configuration because it can detect hidden flaws better and has a substantially greater measurement range. The coplanar configuration is recommended if its measurement range is adequate and if flaws (other than seams) can be visually detected and appropriately tested.

3. The number of small-loop transmitting antenna locations should be increased so that successive test points along seams are never more than 2 ft apart. (Test points around penetrations such as air vents, power line filter boxes, and signal line filter boxes

[27] *Document Review, Standard Shielding Effectiveness Test Methods*, Technical Memo TM-19, The Boeing Company, Huntsville, AL (U.S. Army Corps of Engineers, 31 May 1972); *Measurement of Electromagnetic Shielding Effectiveness—A Review of Present-Day Technology*, IRT 8194-017, prepared by IRT Corporation for Defense Nuclear Agency (16 January 1980); *Recommended Test Procedure for the Measurement of Electromagnetic Shielding Effectiveness of High Performance Shielded Enclosures*, IRT 8494-016-1 (IRT Corporation, 21 March 1980); R. G. McCormack, *Selection of Recommended Electromagnetic/Radio Frequency Interference Shielding Effectiveness Test Procedures for Military Tactical Shelters*, ESL-TR-80-01, prepared by the U.S. Army Construction Engineering Research Laboratory (Engineering and Services Laboratory, Air Force Engineering and Services Center, January 1980).

[28] R. G. McCormack, *Selection of Recommended Electromagnetic/Radio Frequency Interference Shielding Effectiveness Test Procedures for Military Tactical Shelters*, ESL-TR-80-01, prepared by the U.S. Army Construction Engineering Research Laboratory (Engineering and Services Laboratory, Air Force Engineering and Services Center, January 1980).

should not be more than 1 ft apart.) If this becomes too time consuming for large shelters, the large-loop test of IEEE 299 (or a commercially available seam leak detector) may be used to locate the points of maximum signal leakage. The small-loop test may then be performed opposite these points to determine worst-case shileding effectiveness.

4. The small-loop magnetic field test need not be performed at frequencies below 200 kHz unless the shelter has specific shielding needs below that frequency.

5. Selection of the number of frequencies at which small-loop magnetic field testing is to be done in the 200-kHz to 20-MHz range should be based on shielding criticality, advance knowledge of the shelter's future subjection to specific electromagnetic interference (EMI) threats, and the desired overall test reliability.

6. Periodic maintenance testing for magnetic field shielding effectiveness should use either the large-loop test specified in IEEE 299 or a commercially available seam leak detector to first locate points of maximum leakage. These points should then be tested using the small-loop test at 200 kHz to determine worst-case shielding effectiveness.

7. If both antennas can be kept well away from other interfering structures when the ultra-high frequency (UHF) tests (300 MHz to 1 GHz) are performed, the reference signal should be taken using a calculated spacing of the receiving antenna from the reflecting wall. The calculated spacing is one-twelfth of a wavelength.

8. Selection of test frequencies within the 30-MHz to 10-GHz range should be based on the desired test reliability and on engineering judgment. If shielding is not highly critical to the shelter mission, a single frequency within this range is sufficient; a test frequency of 3 GHz is recommended for periodic maintenance tests. If shielding is critical, then the test frequencies specified in MIL-S-55286C (EL) for the S-280 shelter are recommended (400 MHz, 1 GHz, and 10 GHz). Furthermore, if shielding is critical and if it is known that the shelter will be subjected to high-level EMI/RFI at specific frequencies, then additional testing should be done at these particular frequencies.

9. A horn transmitting antenna may be used for microwave tests if it is needed to increase the measurement range.

Considering the findings presented in Chapters 3 and 4 and CERL's experience in EMP testing, the specifications listed in IEEE 299, with the modifications listed above, are recommended for low-cost methods of assuring continuing EMP hardness. However, it is further recommended that maximum use be made of either the IEEE 299 large-loop test or seam leak testers. In addition, a series of test programs should be pursued in which shelters are initially submitted to threat-level EMP tests and to the IEEE 299 tests recommended here, but then followed by extensive seam leak or IEEE 299 large-loop tests; this method will produce test data histories showing the relative merit of these low-frequency approaches. It is believed that if EMP testing is used as a base with corresponding seam leak test data, deterioration in EMP hardness will be demonstrated by a deterioration in seam leak data.

7 CONCLUSIONS

This report has evaluated the analytical techniques applied in the past to convert CW shielding effectiveness test data to values meaningful for EMP radiation. Extension of the Shelkunoff transmission line theory of shielding to slotted shielding, as proposed by Monroe, yields inaccurate results, especially for test loops. A better technique is the Dipole-Moment Approximation, which gives accurate predictions for electrically small slots. Use of the plane wave spectrum approach, as proposed by Villaseca, along with Huygen's principle, produces results that are in good agreement with the experimental results.

This evaluation has also produced recommendations for state-of-the-art CW test techniques for evaluating the EMP hardness of tactical shelters. These include:

1. Use the specifications listed in IEEE 299, with modifications as listed on pp 30 through 31.

2. Make maximum use of the IEEE 299 large-loop test or seam leak testers.

REFERENCES

Atkins, H. E., R. E. Evans, B. J. Gay, H. L. Holt, and A. R. Wright, *Safeguard Tactical Ground Facilities EMP/RFI Facilities Acceptance Construction/ Installation Test Plan–Grand Forks*, prepared by the Boeing Company (U.S. Army Engineer Division, Huntsville, 6 January 1972).

Bannister, P. R., "Further Notes for Predicting Shielding Effectiveness for the Plane Shield Case." *IEEE Transactions on Electromagnetic Compatibility*, Vol EMC-11, No. 2 (May 1969).

Booker, H. G., and P. L. Clemmou, *Proceedings of IEEE*, Vol 97, Part III (1957), pp 11-17.

Butler, C. M., "Dipole Moment Approximation and Polarizabilities," Section 2.1.3.2 in *EMP Interaction Principles, Techniques, and Reference Data*, EMP Interaction 2-1, AFWL-TR-80-402 (Air Force Weapons Lab, Air Force Systems Command, December 1980).

Butler, C. M., Y. Rahmat-Samii, and R. Mittra, "Electromagnetic Penetration Through Apertures in Conducting Surfaces," *IEEE Trans. on Antennas and Propagation*, Vol AP-26, No. 1 (January 1978), pp 82-93.

Continuous Wave (CW) Test Plan for Selected PACOM Assets, IRT 8206-007 (Draft) (IRT Corporation, 6 April 1981).

Document Review, Standard Shielding Effectiveness Test Methods, Technical Memo TM-19, The Boeing Company, Huntsville, AL (U.S. Army Corps of Engineers, 31 May 1972).

EMP Protection for Emergency Operating Centers TR-61A (Department of Defense, July 1972).

Finei, A. G., H. M. Fowles, and P. R. Trybus, *Ground Based C^3 Facilities Hardening and Validation*, GPC^3-3-MRC-064 (Mission Research Corporation, November 1980).

Harrington, R. F., *Time-Harmonic Electromagnetic Fields* (McGraw-Hill Book Company, Inc., 1961), p 110.

McCormack, R. G., *Selection of Recommended Electromagnetic/Radio Frequency Interference Shielding Effectiveness Test Procedures for Military Tactical Shelters*, ESL-TR-80-01, prepared by the U.S. Army Construction Engineering Research Laboratory (Engineering and Services Laboratory, Air Force Engineering and Services Center, January 1980).

Measurement of Electromagnetic Shielding Effectiveness–A Review of Present-Day Technology, IRT 8194-017, prepared by IRT Corporation for Defense Nuclear Agency (16 January 1980).

Military Standard Attenuation Measurements for Enclosures, Electromagnetic Shielding for Electronic Test Purposes, Method of, MIL-STD-285 (Department of Defense, 25 June 1956).

Mittra, R., "Cavity Excitation via Apertures," *EMP Interaction: Principles, Techniques and Reference Data*, Ch 2.3.2.1, K. S. H. Lee, ed. (Air Force Systems Command, December 1980). pp 522-523.

Monroe, R. L., *EMP Shielding Effectiveness and MIL-STD-285*, HDL-TR-1636/AD771997 (Harry Diamond Laboratories, U.S. Army Materiel Command, July 1973).

Moser, J. R., "Low-Frequency Shielding of a Circular Loop Electromagnetic Field Source," *IEEE Transactions on Electromagnetic Compatibility*, Vol EMC-9, No. 1 (March 1969).

Moser, J. R., "Low-Frequency Shielding of a Circular Loop Electromagnetic Field Source," *IEEE Transactions on Electromagnetic Compatibility*, Vol EMC-11, No. 2 (May 1969).

Proposed IEEE Recommended Practice for Measurement of Shielding Effectiveness of High-Performance Shielding Enclosures, IEEE 299 (Institute of Electrical and Electronics Engineers [IEEE] 299, June 1969).

Proposed Revision of IEEE Recommended Practice for Measurement of Shielding Effectiveness of High Performance Shielding Enclosures (Draft) (IEEE).

Recommended Test Procedure for the Measurement of Electromagnetic Shielding Effectiveness of High Performance Shielded Enclosures, IRT 8494-016-1, (IRT Corporation, 21 March 1980).

Trybus, P. R., *National Security Agency Specification for R. F. Shielded Enclosures for Communications Equipment: General Specification*, NSA 65-6 (National Security Agency, 30 October 1964).

Tyras, George, *Radiation and Propagation of Electromagnetic Waves* (Academic Press, 1969), pp 40–43.

Villaseca, E., C. Davis, W. Blackwood, and W. Getson, *An Investigation of the Validity of Applying MIL-STD-285 to EMP Shielding Effectiveness,"* ADA051889, prepared by Harris Corp. Electronics System Division (Defense Nuclear Agency, 15 April 1977).

Yung, E. K., S. W. Lee, and R. Mittra, "Penetration of an EM Wave into a Cylindrical Cavity and the Current Induced on a Wire Inside," *AEU*, Band 33, Heft 4, (1979), pp 149-156.

APPENDIX A: ELECTROMAGNETIC COUPLING THROUGH MULTILAYERED SHIELDS FOR AN ARBITRARY ILLUMINATING SOURCE

Introduction

The EMP/EMI testing of shelters requires measuring the coupling between two test antennas. One is located external to the enclosure, and the other is placed in the interior region. Typically, the test antennas are small loops or dipoles, and they can often be modeled as elemental magnetic or electric dipoles. While formulas for computing the coupling between two coaxial loops in the presence of planar multi-layered shields can be found in the literature,[29] general formulas for arbitrary orientation of the loop or dipole antennas are not readily available. The approach documented here is based on the plane wave spectral representation; this method is useful for calculating the shielding effectiveness of multi-layered sheets under very general test conditions. Since the method is capable of handling arbitrary incident fields, loops or dipoles oriented in arbitrary directions can be accommodated.

The method proceeds by considering an interface between two media (see Figure A1) and expresses the incident fields in terms of a plane wave spectrum. The next step relates the fields in the input and output terminal planes (arbitrarily defined on two sides of the junction of two dissimilar media) via a transfer matrix, T, which is independent of the nature of the incident field. The elements of T are expressible in terms of the constitutive parameters of the two media and the location of the terminal planes. The multiple-junction case is handled rather simply by cascading the T-matrices for the individual interfaces; no limitation is placed on the number of layers in the shield.

[29] R. L. Monroe, *EMP Shielding Effectiveness and MIL-STD-285*, HDL-TR-1636/AD771997 (Harry Diamond Laboratories, U.S. Army Materiel Command, July 1973); E. Villaseca, C. Davis, W. Blackwood, and W. Getson, *An Investigation of the Validity of Applying MIL-STD-285 to EMP Shielding Effectiveness*, ADA051889, prepared by Harris Corp. Electronics System Division (Defense Nuclear Agency, 15 April 1977); J. R. Moser, "Low-Frequency Shielding of a Circular Loop Electromagnetic Field Source," *IEEE Transactions on Electromagentic Compatibility*, Vol EMC-11, No. 2 (May 1969).

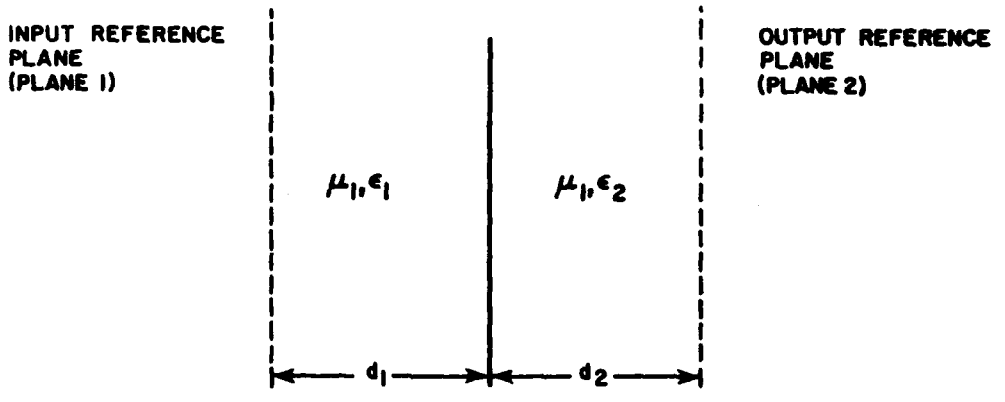

Figure A1. Media interface with input and output reference planes.

The following section presents the derivation of the T matrix that relates the transformation of fields between the input and output terminal planes 1 and 2 in Figure A1.

Derivation of the Transformation Matrix, T

The Cartesian coordinate system, with the z-axis normal to the interface, appears to be the obvious choice for expressing the fields for the interface problem shown in Figure A1. With this choice for axes, there are four components of the E-field (E_x^a, E_y^a, E_x^b, E_y^b) at plane 1 and similar ones at plane 2; the superscripts a and b refer to incoming and outgoing fields that must be related by a 4 x 4 matrix. However, considerable simplification results if an alternative choice is made for the coordinate system in which the various fields are represented. Let us consider an incident plane wave and define the plane of incidence as that containing the wave normal and the normal to the interface. The planes of reflection and transmission can be defined similarly. We then resolve the incident E and H fields into two components: one is parallel to the plane of incidence, and the other is perpendicular. These components are labeled with subscripts $\parallel$ and $\perp$, respectively. Then we can show that these two components propagate independently and remain uncoupled throughout the process of reflection and transmission. It is important to observe that if we were to work with the conventional x, y, z system, there would generally be coupling between the various components. Thus, for convenience, it is useful to introduce the notation where the superscript a indicates incoming waves into the planes 1 and 2, while the superscript b indicates outgoing waves. Finally, the superscripts 1 and 2 would refer to the fields at the corresponding terminal planes and the $\tilde{}$ on top would indicate Fourier transforms.

The plane wave spectrum representations for the various field components take the form:

$$\underset{\perp}{E^{1a}} = \iint \underset{\perp}{\tilde{E}^{1a}}\ (\alpha,\beta)\, e^{j[\alpha x + \beta y - \gamma_1(z+d_1)]}\, d\alpha\, d\beta \quad \text{[Eq A1]}$$

$$\underset{\perp}{E^{1b}} = \iint \underset{\perp}{\tilde{E}^{1b}}\ (\alpha,\beta)\, e^{j[\alpha x + \beta y - \gamma_1(z+d_1)]}\, d\alpha\, d\beta \quad \text{[Eq A2]}$$

$$\underset{\perp}{E^{2a}} = \iint \underset{\perp}{\tilde{E}^{2a}}\ (\alpha,\beta)\, e^{j[\alpha x + \beta y - \gamma_2(z+d_2)]}\, d\alpha\, d\beta \quad \text{[Eq A3]}$$

$$\underset{\perp}{E^{2b}} = \iint \underset{\perp}{\tilde{E}^{2b}}\ (\alpha,\beta)\, e^{j[\alpha x + \beta y - \gamma_2(z+d_2)]}\, d\alpha\, d\beta \quad \text{[Eq A4]}$$

where $\gamma_{1,2} = \sqrt{k_{1,2}^2 - \alpha^2 - \beta^2}$, $k_{1,2}^2 = \omega^2 \mu \epsilon_{1,2}$, and d_1, d_2 are distances of the terminal planes from the interface of the two media.

Similar expressions can be written for the field's parallel components. However, these fields can be analyzed totally independently because they are uncoupled.

The next step applies the curl equations to obtain the corresponding magnetic field components and applies the continuity conditions of the tangential fields at the interface. Instead of having to work in the spatial domain, one can apply the continuity conditions equally well in the spectral domain, obtaining:

[Eq A5]

$$E^{1a} e^{j\gamma_1 d_1} + E^{1b} e^{-j\gamma_1 d_1} = E^{2a} e^{j\gamma_2 d_2} + E^{2b} e^{-j\gamma_2 d_2}$$

$$\sqrt{\epsilon/\mu}\,[E^{1a} e^{j\gamma_1 d_1} - E^{1b} e^{-j\gamma_1 d_1}]\cos\theta_1 =$$

$$\sqrt{\epsilon_2/u_2}\,[E^{2a} e^{j\gamma_2 d_2} - E^{2b} e^{-j\gamma_2 d_2}]\cos\theta_2$$

where

θ_1 = angle between k_1 and the normal to the surface, vector $\hat{z}$,

θ_2 = angle between k_2 and the normal to the surface, vector $\hat{z}$, and $\cos\theta_1 = \dfrac{k_1 \cdot \hat{z}}{|k_1|}$, $\cos\theta_2 = \dfrac{k_2 \cdot \hat{z}}{|k_2|}$.

We have dropped the subscript $\perp$ and the $\tilde{}$ on top, which are implicit.

The transfer matrix between the terminal planes 1 and 2 is defined as:

$$\underset{\perp}{\{E^2\}} = [T]\ \underset{\perp}{\{E^1\}} \quad \text{[Eq A6]}$$

Following the steps given above, one can obtain the expression for the transfer matrix, which, for the $\perp$ fields, the elements of which are given by:

$$T_{\perp_{11}} = \frac{\sqrt{\epsilon_2}\cos\theta_2 - \sqrt{\epsilon}\cos\theta_1}{2P_2}\, e^{j(\gamma_1 d_1 - \gamma_2 d_2)}$$

$$T_{\perp_{12}} = \frac{\sqrt{\epsilon_2}\cos\theta_2 + \sqrt{\epsilon}\cos\theta_1}{2P_2}\, e^{-j(\gamma_2 d_2 + \gamma_1 d_1)}$$

$$T_{\perp_{21}} = \frac{\sqrt{\epsilon_2}\cos\theta_2 + \sqrt{\epsilon}\cos\theta_1}{2P_2}\, e^{j(\gamma_1 d_1 + \gamma_2 d_2)}$$

$$T_{\perp_{22}} = \frac{\sqrt{\epsilon_2}\cos\theta_2 - \sqrt{\epsilon}\cos\theta_1}{2P_2} e^{j(\gamma_2 d_2 - \gamma_1 d_1)}$$

where $P_2 = \sqrt{\epsilon_2}\cos\theta_2$.

Similarly, one can derive the transfer matrix, $T_{||}$, for the parallel component. Its elements are given by:

$$T_{||_{11}} = \frac{\sqrt{\epsilon_1}\cos\theta_2 - \sqrt{\epsilon_2}\cos\theta_1}{2P_2} e^{j(\gamma_1 d_1 - \gamma_2 d_2)},$$

$$T_{||_{12}} = \frac{\sqrt{\epsilon_1}\cos\theta_2 + \sqrt{\epsilon_2}\cos\theta_1}{2P_2} e^{-j(\gamma_1 d_1 + \gamma_2 d_2)}$$

$$T_{||_{21}} = \frac{\sqrt{\epsilon_1}\cos\theta_2 + \sqrt{\epsilon_2}\cos\theta_1}{2P_2} e^{j(\gamma_1 d_1 + \gamma_2 d_2)}$$

$$T_{||_{22}} = \frac{\sqrt{\epsilon_2}\cos\theta_1 - \sqrt{\epsilon_2}\cos\theta_1}{2P_2} e^{j(\gamma_2 d_2 - \gamma_1 d_1)}$$

For the multi-layered case, the individual T-matrices for each of the interfaces may be cascaded to derive a composite T-matrix for the entire shield. Then, the transmitted fields in the extreme right region can be related to those in the extreme left using the composite T-matrix. Finally, the incident fields in the extreme left region can be assumed known, and one can use the fact that the incident field is identically zero in the extreme right region. Hence, the reflected and transmitted fields in the extreme left and extreme right regions, respectively, can be readily calculated from the knowledge of the composite T-matrix and the incident fields.

Determination of Incident Fields

This section briefly describes the method for determining the fields generated by elemental electric and magnetic dipole sources. We consider four different cases:

1. Electric dipole oriented along the z-direction
2. Electric dipole oriented along the x-direction
3. Magnetic dipole oriented along the z-direction
4. Magnetic dipole oriented along the x-direction.

All of these problems are most conveniently solved in the transform or spectral domain, where the wave equations for electric or magnetic vector potentials become algebraic.

Electric Dipole Oriented Along Z-Direction

For a z-oriented dipole source, the z-component of the electric vector potential A_z satisfies the wave equation:

$$\nabla^2 A_z + k^2 A_z = -Idl\,\delta(x-x')\,\delta(y-y')\,\delta(x-x') \qquad \text{[Eq A7]}$$

where Idl is the dipole moment of the elemental dipole. This equation for A_z can be solved using the transform technique to yield:

$$A_z(x,y,z) = \frac{Idl}{2(2\pi)^2}\iint_{-\infty}^{\infty} \frac{-j}{\sqrt{k^2-\alpha^2-\beta^2}} \cdot e^{j[\alpha(x-x')+\beta(y-y')-\sqrt{k^2-\alpha^2-\beta^2}\,|z-z'|]}\,d\alpha d\beta$$

From Maxwell's equations, we have:

$$H_x = \frac{\partial A_z}{\partial y} \qquad E_x = \frac{+1}{j\omega\epsilon}\frac{\partial^2 A_z}{\partial z \partial x} \qquad \text{[Eq A8]}$$

$$H_y = \frac{\partial A_z}{\partial x} \qquad E_y = \frac{1}{j\omega\epsilon}\frac{\partial^2 A_z}{\partial z \partial y} \qquad \text{[Eq A9]}$$

The expressions for the various components of electric and magnetic fields are given in Eqs A10–A14.

[Eq A10]

$$H_x = \frac{Idl}{2(2\pi)^2}\iint_{-\infty}^{\infty} \frac{\beta}{\sqrt{k^2-\alpha^2-\beta^2}} e^{j[\alpha(x-x')+\beta(y-y')-\gamma|z-z'|]}\,d\alpha d\beta$$

[Eq A11]

$$H_y = \frac{-Idl}{2(2\pi)^2}\iint_{-\infty}^{\infty} \frac{+\alpha}{\sqrt{k^2-\alpha^2-\beta^2}} e^{j[\ ]}\,d\alpha\,d\beta;\ [\ ] =$$

$$[\alpha(x-x')+\beta(y-y')-\gamma|z-z'|]$$

$$E_x = \frac{-Idl}{(j\omega\epsilon)2(2\pi)^2}\iint_{-\infty}^{\infty} j\,\alpha\, e^{j[\ ]}\,d\alpha\,d\beta \qquad \text{[Eq A12]}$$

$$E_y = \frac{-Idl}{(j\omega\epsilon)2(2\pi)^2}\iint_{-\infty}^{\infty} j\,\beta\, e^{j[\ ]}\,d\alpha\,d\beta \qquad \text{[Eq A13]}$$

$$E_z = \frac{-Idl}{(j\omega\epsilon)2(2pi)^2}\iint_{-\infty}^{\infty} \frac{j(\alpha^2+\beta^2)}{\sqrt{k^2-\alpha^2-p^2}} e^{j[\ ]}\,d\alpha\,d\beta \qquad \text{[Eq A14]}$$

Electric Dipole Oriented Along x-Direction

For a dipole oriented along the x direction, the field components are given by:

[Eq A15]

$$H_y = \frac{-Idl}{2(2\pi)^2}\iint_{-\infty}^{\infty} e^{j[\alpha(x-x')+\beta(y-y')-\gamma|z-z'|]}\,d\alpha\,d\beta$$

$$H_z = \frac{-Idl}{2(2\pi)^2}\iint_{-\infty}^{\infty} \frac{\beta}{\sqrt{k^2-\alpha^2-\beta^2}}\,e^{j[\ ]}\,d\alpha\,d\beta \qquad \text{[Eq A16]}$$

$$E_x = \frac{-Idl}{j\omega\varepsilon 2(2\pi)^2}\iint_{-\infty}^{\infty} \frac{j(k^2-\alpha^2)}{\sqrt{k^2-\alpha^2-\beta^2}}\,e^{j[\ ]}\,d\alpha\,d\beta \qquad \text{[Eq A17]}$$

$$E_y = \frac{Idl}{(j\omega\varepsilon)2(2\pi)^2}\iint_{-\infty}^{\infty} \frac{j\alpha\beta}{\sqrt{k^2-\alpha^2-\beta^2}}\,e^{j[\ ]}\,d\alpha\,d\beta \qquad \text{[Eq A18]}$$

$$E_z = \frac{-Idl}{(j\omega\varepsilon)2(2\pi)^2}\iint_{-\infty}^{\infty} j\alpha\,e^{j[\ ]}\,d\alpha\,d\beta \qquad \text{[Eq A19]}$$

Magnetic Dipole Oriented Along the z-Direction

For a z-oriented magnetic dipole of moment Kdl, we solve first for the magnetic vector potential F_z and derive the E- and H-fields from this potential. The field expressions are:

[Eq A20]

$$E_x = \frac{Kdl}{2(2\pi)^2}\iint_{-\infty}^{\infty} \frac{-\beta}{\sqrt{k^2-\alpha^2-\beta^2}}\,e^{j[\alpha(x-x')+\beta(y-y')-\gamma|z-z'|]}\,d\alpha\,d\beta$$

$$E_y = \frac{Kdl}{2(2\pi)^2}\iint_{-\infty}^{\infty} \frac{\alpha}{\sqrt{k^2-\alpha^2-\beta^2}}\,e^{j[\ ]}\,d\alpha\,d\beta \qquad \text{[Eq A21]}$$

$$H_x = \frac{-Kdl}{j\omega\mu 2(2\pi)^2}\iint_{-\infty}^{\infty} j\alpha\,e^{j[\ ]}\,d\alpha\,d\beta \qquad \text{[Eq A22]}$$

$$H_y = \frac{-Kdl}{(j\omega\mu)2(2\pi)^2}\iint_{-\infty}^{\infty} j^p\,e^{j[\ ]}\,d\alpha\,d\beta \qquad \text{[Eq A23]}$$

$$H_z = \frac{-Kdl}{(j\omega\mu)2(2\pi)^2}\iint_{-\infty}^{\infty} \frac{j(\alpha^2+\beta^2)}{\sqrt{k^2-\alpha^2-\beta^2}}\,e^{j[\ ]}\,d\alpha\,d\beta \qquad \text{[Eq A24]}$$

Magnetic Dipole Oriented Along the x-Direction

Finally, for an x-oriented magnetic dipole of moment Kdl, the corresponding expressions are:

[Eq A25]

$$E_y = \frac{Kdl}{2(2\pi)^2}\iint_{-\infty}^{\infty} e^{j[\alpha(x-x')+\beta(y-y')-\gamma|z-z'|]}\,d\alpha\,d\beta$$

$$E_z = \frac{Kdl}{2(2\pi)^2}\iint_{-\infty}^{\infty} \beta\,e^{j[\ ]}\,d\alpha\,d\beta \qquad \text{[Eq A26]}$$

$$H_x = \frac{-Kdl}{(j\omega\mu)2(2\pi)^2}\iint_{-\infty}^{\infty} \frac{j(k^2-\alpha^2)}{\sqrt{k^2-\alpha^2-\beta^2}}\,e^{j[\ ]}\,d\alpha\,d\beta \qquad \text{[Eq A27]}$$

$$H_y = \frac{-Kdl}{(j\omega\mu)2(2\pi)^2}\iint_{-\infty}^{\infty} \frac{-j\alpha\beta}{\sqrt{k^2-\alpha^2-\beta^2}}\,e^{j[\ ]}\,d\alpha\,d\beta \qquad \text{[Eq A28]}$$

$$H_z = \frac{-Kdl}{(j\omega\mu)2(2\pi)^2}\iint_{-\infty}^{\infty} j\alpha\,e^{j[\ ]}\,d\alpha\,d\beta \qquad \text{[Eq A29]}$$

Once again, one can work initially in the transform domain to carry out the multiplication of the T-matrices and use the incident field components to derive the transmitted fields, also in the transform domain. These can then be Fourier-inverted, and the field coupling into another dipole at the receiving end may be computed by taking a dot product of the appropriate field component with the electric or magnetic dipole moment.

Coordinate Transformation

Let us consider the problem of coordinate transformation from the x, y, z coordinate system to the system defined by the orthogonal triad consisting of the wave normal and the vectors parallel and perpendicular to the plane of incidence. To accomplish the transformation, we use a rotation matrix R. For the E fields, the matrix R is defined by:

$$\begin{bmatrix} E_{11} \\ E \\ E_k \end{bmatrix} = R \begin{vmatrix} E_x \\ E_y \\ E_z \end{vmatrix} \qquad \text{[Eq A30]}$$

$$R = \begin{bmatrix} -\sin\theta & \cos\theta & 0 \\ -\cos\theta\cos\phi & -\cos\theta\sin\phi & \sin\theta \\ \sin\theta\cos\phi & \sin\theta\sin\phi & \cos\theta \end{bmatrix} \qquad \text{[Eq A31]}$$

where:

$$\cos\theta = \frac{\bar{k}\cdot\hat{z}}{|k|}$$

$$\sin\theta = \sqrt{1-\frac{\bar{k}\cdot\hat{z}^2}{|k|}}$$

$$\cos\phi = \frac{\bar{k}\cdot\hat{x}}{\sqrt{|\bar{k}|^2-(\bar{k}\cdot\hat{z})^2}}$$

$$\sin\phi = \frac{\bar{k}\cdot\hat{x}}{\sqrt{|\bar{k}|^2-(\bar{k}\cdot\hat{z})^2}}$$

APPENDIX B:
COMPUTER PROGRAMS: MULSH, APRAD, *SLOT, SLITCP, and SLITCA*

```
      PROGRAM SLOT2(INPUT,OUTPUT,TAPE5=INPUT,TAPE6=OUTPUT)
      COMPLEX RKD,RKL,RKDPO,RKLPO
      COMPLEX ZSL,TOP,ZD,ZDT,ZDB,ZL,ZLT,ZLB
      PI=3.1415926536
      WRITE(6,100)
  100 FORMAT(/,2X,*LARGE SLOT=01,SMALL SLOT=00*)
      READ(5,200)ISIZ
  200  FORMAT(I2)
      IF(ISIZ .EQ. 1) GO TO 10
      SL=0.25
      A=7.9375E-4
      GO TO 20
   10 SL=0.5
      A=1.5875E-3
   20 CONTINUE
      R=.3048
      WRITE(6,101)
  101 FORMAT(/,2X,*ENTER START FREQ. (MHZ)*)
      READ(5,201)FSTART
  201 FORMAT(F14.2)
      FR=FSTART
      WRITE(6,107)
  107 FORMAT(/,2X,*ENTER MAX FREQ. (MHZ)*)
      READ(5,203)FRMAX
  203 FORMAT(F14.2)
      FRINC=10.**(.125)
      IFLP=0
 1234 F=FR*1.E+6
      IFLP=IFLP+1
      ALAM=3.0E08/F
      BETA=2.*PI/ALAM
      TBL=2.*BETA*SL
      FBL=4.*BETA*SL
      SOTBL=0.0
      SOFBL=0.0
      SITBL=0.0
      SIFBL=0.0
C  CALCULATE SOTBL
      N=0
   30 N=N+1
      ITN=2*N
      CALL FACT(ITN,ITNF)
  501 FORMAT(I4,I4)
      TERM=(-1.)*((-1.)**N)*((TBL)**ITN)/(ITN*ITNF)
      SOTBL=SOTBL+TERM
      IF(N .LT. 5) GO TO 30
C  CALCULATE SOFBL
      N=0
   40 N=N+1
      ITN=2*N
      CALL FACT(ITN,ITNF)
      TERM=(-1.)*((-1.)**N)*((FBL)**ITN)/(ITN*ITNF)
      SOFBL=SOFBL+TERM
      IF(N .LT. 5) GO TO 40
```

```
C  CALCULATE SITBL
       N=-1
  50   N=N+1
       ITNPO=2*N+1
       CALL FACT(ITNPO,ITNPOF)
       TERM=((-1.)**N)*((TBL)**ITNPO)/(ITNPO*ITNPOF)
       SITPL=SITPL+TERM
       IF(N .LT. 4) GO TO 50
C  CALCULATE SIFBL
       N=-1
  60   N=N+1
       ITNPO=2*N+1
       CALL FACT(ITNPO,ITNPOF)
       TERM=((-1.)**N)*((FBL)**ITNPO)/(ITNPO*ITNPOF)
       SIFBL=SIFBL + TERM
       IF(N .LT. 4) GO TO 60
       RAD=15.*((2.+2.*COS(TBL))*SOTBL
      &-COS(TBL)*SOFBL-2.*SIN(TBL)*SITBL
      &+SIN(TBL)*SIFBL)
       ZO=120.*(ALOG(SL/A)-1.0-.5*ALOG(2.*SL/ALAM))
       GAM=2.0*RAD/ZO
       EPG=EXP(GAM)
       EMG=1./EPG
       EPTG=EXP(2.*GAM)
       EMTG=1./EPTG
       SHTG=(EPTG-EMTG)/2.
       CHG=(EPG+EMG)/2.
       CHGS=CHG**2
       COSSBL=(COS(BETA*SL))**2
 502   FORMAT(E14.7,E14.7)
       RCD=(ZO/2.)*(SHTG/(CHGS-COSSBL))
       XCD=(ZO/2.)*((-1.)*SIN(TBL)/(CHGS-COSSBL))
       RCDS=RCD**2
       XCDS=XCD**2
       TOP=CMPLX(RCD,(-1.)*XCD)
       BOT=RCDS+XCDS
       ZSL=(((377.)**2)/4.)*(TOP/BOT)
       ZMAG=CABS(ZSL)
 102   FORMAT(/,2X,*ZSL=*,E14.4)
C  CALCULATE DIPOLE IMPEDANCE
       ZRDT=1.-(BETA**2)*(R**2)
       ZIDT=BETA*R
       ZRDB=(-1.)*(BETA**2)*(R**2)
       ZIDB=ZIDT
       ZDT=CMPLX(ZRDT,ZIDT)
       ZDB=CMPLX(ZRDB,ZIDB)
       ZD=(377.)*(ZDT/ZDB)
       ZDMAG=CABS(ZD)
C  CALCULATE LOOP IMPEDANCE
       ZRLT=ZRDB
       ZILT=ZIDT
       ZRLB=ZRDT
       ZILB=ZIDT
       ZLT=CMPLX(ZRLT,ZILT)
       ZLB=CMPLX(ZRLB,ZILB)
       ZL=(377.)*(ZLT/ZLB)
       ZLMAG=CABS(ZL)
```

```
 104  FORMAT(/,2X,3E14.4)
C  CALCULATE SHIELDING EFFECTIVENESS FOR DIPOLE
      RKD=ZD/ZSL
      RKDPO=RKD+1.0
      DKM=CABS(RKD)
      DKMO=CABS(RKDPO)
      SED=20.*ALOG10(DKMO**2/(4.*DKM))
C  CALCULATE SHIELDING EFFECTIVENESS FOR LOOP
      RKL=ZL/ZSL
      RKLPO=RKL+1.0
      EKM=CABS(RKL)
      EKMO=CABS(RKLPO)
      SEL=20.*ALOG10(EKMO**2/(4.*EKM))
      IF(IFLP .GT. 1) GO TO 77
      WRITE(6,105)
 105  FORMAT(20X,*FREQ(HZ)*,10X,*SE DIPOLE*,10X,*SE LOOP*,//)
  77  CONTINUE
      WRITE(6,106)F,SED,SEL
 106  FORMAT(18X,E10.3,8X,E10.3,9X,E10.3)
      FR=FR*FRINC
      IF(FR .LE. FRMAX) GO TO 1234
      WRITE(6,103)
 103  FORMAT(/,2X,*CONTINUE? Y=1, N=0*)
      READ(5,202)IROT
 202  FORMAT(I2)
      IF(IROT .EQ. 1) GO TO 20
      STOP
      END
      SUBROUTINE FACT(N,NFACT)
      NFACT=N
      IF(N .EQ. 0)NFACT=1
      M=N
  10  CONTINUE
      M=M-1
      IF(M.EQ.1)GO TO 20
      IF(M.EQ.0)GO TO 20
      NFACT=NFACT*M
      GO TO 10
  20  CONTINUE
      RETURN
      END
```

```
      PROGRAM SLITCP(INPUT,OUTPUT,TAPE5=INPUT,TAPE6=OUTPUT)
      REAL LAM,HREFR,HREFI,HREFM,HRI,HRR,HTR,HTI,HDTZM
      COMPLEX HR,HTHE,HX,ARG,HDZ,HDZT
      DIMENSION XP(5),DXP(5)
      PI=3.1415926536
      WRITE(6,102)
  102 FORMAT(/,2X,*LARGE SLOT=01, SMALL SLOT=00*)
      READ(5,202)ISLOT
  202 FORMAT(I2)
      WRITE(6,100)
  100 FORMAT(/,2X,*ENTER START FREQ (MHZ)*)
      READ(5,200)FR
  200 FORMAT(E10.1)
      WRITE(6,101)
  101 FORMAT(/,2X,*ENTER MAX FREQ (MHZ)*)
      READ(5,201)FRMAX
  201 FORMAT(E10.1)
      DELT=.125
      FRINC=10.**DELT
      WRITE(6,103)
  103 FORMAT(//,30X,*FREQ (HZ)*,10X,*SE (DB)*,//)
C  BEGIN FREQ LOOP
   10 F=FR*1.E+6
      LAM=3.0E08/F
C  CALCULATE REF H FIELD ON AXIS AT 3 FEET
      BETA=2.*PI/LAM
      R=.9144
      BETAR=BETA*R
      HREFR=COS(BETAR)-SIN(BETAR)/BETAR-COS(BETAR)/(BETAR**2)
      HREFI=SIN(BETAR)/(BETAR**2)-SIN(BETAR)-COS(BETAR)/BETAR
      HREFR=HREFR*(BETA**2)/(4.*PI*R)
      HREFI=HREFI*(BETA**2)/(4.*PI*R)
      HREFM=SQRT(HREFR**2+HREFI**2)
      IF(ISLOT .EQ. 1) GO TO 20
      IF(ISLOT .EQ. 0) GO TO 30
   20 XP(1)=.25
      XP(2)=.5
      XP(3)=-.25
      XP(4)=-.5
      XP(5)=0.0
      DXP(1)=DXP(3)=DXP(5)=.25
      DXP(2)=DXP(4)=.125
      DY=.0015875
      EL=1.0
      AMX=.02132
      GO TO 40
   30 XP(1)=.125
      XP(2)=.25
      XP(3)=-.125
      XP(4)=-.25
      XP(5)=0.0
      DXP(1)=DXP(3)=DXP(5)=.125
      DXP(2)=DXP(4)=.0625
      DY=.00079375
      EL=0.5
      AMX=.002665
```

```
   40  CONTINUE
       HDZT=(0.0,0.0)
       DO 2000 I=1,5
C  CALCULATE HX ALONG SLOT
       Z=.4572
       X=XP(I)
       DX=DXP(I)
       ALPHA=ATAN(X/.4572)
       THETA=PI/2.-ATAN(X/.4572)
       R=.4572/COS(ALPHA)
       BETAR=BETA*R
       HRR=(COS(THETA)/(2.*PI))*((COS(BETAR)/(R**3))
      ++BETA*SIN(BETAR)/(R**2))
       HRI=(COS(THETA)/(2.*PI))*(BETA*COS(BETAR)/(R**2)
      +-SIN(BETAR)/(R**3))
       HR=CMPLX(HRR,HRI)
       HTR=COS(BETAR)-SIN(BETAR)/BETAR-COS(BETAR)/(BETAR**2)
       HTR=HTR*(-1.0)*(BETA**2)*SIN(THETA)/(4.*PI*R)
       HTI=SIN(BETAR)/(BETAR**2)-SIN(BETAR)-COS(BETAR)/BETAR
       HTI=HTI*(-1.0)*(BETA**2)*SIN(THETA)/(4.*PI*R)
       HTHE=CMPLX(HTR,HTI)
       HX=(HR*X)/SQRT(X**2+(.4572)**2)
      ++HTHE*(.4572)/SQRT(X**2+(.4572)**2)
       HX=HX*DX
C  CALCULATE CONTR. TO SHADOW SIDE FIELD
       RMRP=SQRT(X**2+(.4572)**2)
       RMRPM=(-1.0)*RMRP
       ARG=CMPLX(0.0,RMRPM)
       HDZ=6.*AMX*HX*((.4572)**2)*CEXP(ARG)/((RMRP**5)*4.*PI)
 2000 HDZT=HDZT+HDZ
       HDZT=HDZT/(5.0*EL)
       HDZTM=CABS(HDZT)
       SE=20.*ALOG10(HREFM/HDZTM)
       WRITE(6,104)F,SE
  104  FORMAT(30X,E10.3,5X,F10.3)
       FR=FR*FRINC
       IF(FR .LE. FRMAX) GO TO 10
       STOP
       END
C>
```

```
      PROGRAM SLITCA(INPUT,OUTPUT,TAPE5=INPUT,TAPE6=OUTPUT)
      REAL LAM,HREFR,HREFI,HREFM,HRI,HRR,HTR,HTI,HDTZM
      COMPLEX HR,HTHE,HX,ARG,HDZ,HDZT
      DIMENSION XP(4),DXP(4)
      PI=3.1415926536
      WRITE(6,102)
  102 FORMAT(/,2X,*LARGE SLOT=01, SMALL SLOT=00*)
      READ(5,202)ISLOT
  202 FORMAT(I2)
      WRITE(6,100)
  100 FORMAT(/,2X,*ENTER START FREQ (MHZ)*)
      READ(5,200)FR
  200 FORMAT(E10.1)
      WRITE(6,101)
  101 FORMAT(/,2X,*ENTER MAX FREQ (MHZ)*)
      READ(5,201)FRMAX
  201 FORMAT(E10.1)
      DELT=.125
      FRINC=10.**DELT
      WRITE(6,103)
  103 FORMAT(//,30X,*FREQ (HZ)*,10X,*SE (DB)*,//)
C  BEGIN FREQ LOOP
   10 F=FR*1.E+6
      LAM=3.0E08/F
C  CALCULATE REF H FIELD ON AXIS AT 2 FEET
      BETA=2.*PI/LAM
      R=.61
      BETAR=BETA*R
      HREFR=COS(BETAR)/(R**3)+(BETA*SIN(BETAR))/(R**2)
      HREFI=(-1.)*SIN(BETAR)/(R**3)+(BETA*COS(BETAR))/(R**2)
      HREFR=HREFR/(2.*PI)
      HREFI=HREFI/(2.*PI)
      HREFM=SQRT(HREFR**2+HREFI**2)
      IF(ISLOT .EQ. 1) GO TO 20
      IF(ISLOT .EQ. 0) GO TO 30
   20 XP(1)=.25
      XP(2)=.5
      XP(3)=-.25
      XP(4)=-.5
      DXP(1)=DXP(3)=.25
      DXP(2)=DXP(4)=.125
      DY=.0015875
      EL=1.0
      AMX=.02132
      GO TO 40
   30 XP(1)=.125
      XP(2)=.25
      XP(3)=-.125
      XP(4)=-.25
      DXP(1)=DXP(3)=.125
      DXP(2)=DXP(4)=.0625
      DY=.00079375
      EL=0.5
      AMX=.002665
```

```
  40  CONTINUE
      HDZT=(0.0,0.0)
      DO 2000 I=1,4
C  CALCULATE HX ALONG SLOT
      Z=.305
      X=XP(I)
      DX=DXP(I)
      THETA=ATAN(X/.305)
      R=.305/COS(THETA)
      BETAR=BETA*R
      HRR=(COS(THETA)/(2.*PI))*((COS(BETAR)/(R**3))
     ++BETA*SIN(BETAR)/(R**2))
      HRI=(COS(THETA)/(2.*PI))*(BETA*COS(BETAR)/(R**2)
     +-SIN(BETAR)/(R**3))
      HR=CMPLX(HRR,HRI)
      HTR=COS(BETAR)-SIN(BETAR)/BETAR-COS(BETAR)/(BETAR**2)
      HTR=HTR*(-1.0)*(BETA**2)*SIN(THETA)/(4.*PI*R)
      HTI=SIN(BETAR)/(BETAR**2)-SIN(BETAR)-COS(BETAR)/BETAR
      HTI=HTI*(-1.0)*(BETA**2)*SIN(THETA)/(4.*PI*R)
      HTHE=CMPLX(HTR,HTI)
      HX=(HR*X)/SQRT(X**2+(.305)**2)
     ++HTHE*X*(.305)/SQRT((X**2)*(X**2+(.305)**2))
      HX=HX*2.*DX
C  CALCULATE CONTR. TO SHADOW SIDE FIELD
      RMRP=SQRT(X**2+(.305)**2)
      RMRPM=(-1.0)*RMRP
      ARG=CMPLX(0.0,RMRPM)
      HDZ=6.*AMX*HX*(-1.0)*X*(.305)*CEXP(ARG)/((RMRP**5)*4.*PI)
 2000 HDZT=HDZT+HDZ
      HDZT=HDZT/(5.0*EL)
      HDZTM=CABS(HDZT)
      SE=20.*ALOG10(HREFM/HDZTM)
      WRITE(6,104)F,SE
  104 FORMAT(30X,E10.3,5X,F10.3)
      FR=FR*FRINC
      IF(FR .LE. FRMAX) GO TO 10
      STOP
      END
C>
```

```
      PROGRAM MULSH (INPUT,OUTPUT,TAPE5=INPUT,TAPE6=OUTPUT)
      DIMENSION FREQ(100),FLOG(100),SHEF(100),BCD(3),BF(5000),SH(100,10)
      DIMENSION LX(7),LY(7),LM(7),LS(7)
      COMMON/PARAMS/NOPT(7),D(7),SIGR(7),EMUR(7),EPSR(7),DLUP(7),FRCN(7)
     1,NGO,LL(7)
      COMMON/CONSTS/PI,EMUO,EPSO,SIGC
      COMMON/STPCOM/IMAGE(2100)
      COMPLEX EJ, SUMD, CEP, CEM, PROD, TZMD, CE, FACT
      COMPLEX ZIN
      COMPLEX GS(7), TAU(7), PSY(7), HT(7), SZR(7), POLE(7), CSPL(7)
      COMPLEX TRAN(1000), REFL(1000)
C
      PI=3.1415926536
      TP=2.*PI
      ERR=1.E-10
      EMUO=1.26E-6
      EPSO=8.854E-12
      SIGC=5.80E+7
      VL=3.E+8
      EJ=CMPLX(0.,1.)
C
C.....BEGIN PROBLEM LOOP
      KK=0
 1000 CONTINUE
      KK=KK+1
      WRITE(6,100)KK
      CALL IADATA
      MC=NOPT(1)
      MCM=MC-1
      IMAX=NOPT(2)
      IF(IMAX.GT.1000)STOP 1000
      IDBP=NOPT(3)
      IPLT=NOPT(4)
C
      A =DLUP(1)
      DAL = DLUP(2)
      DD = 0.
      DO 5 M=2,MCM
    5 DD=DD+D(M)
      ZMD = D(1)+D(MC)
      RDR = ZMD+DD
C
C.....NUMERATOR INTEGRAL
      RS=A*A+RDR*RDR
      R=SQRT(RS)
      TERM=EMUR(1)*R*R*R/A
C
C.....BESSEL TERMS
      AL=0.
      DO 10 I=1,IMAX
      X=AL*A
      CALL BESJ(X,1,BJ,ERR,IERROR)
      IF(IERROR.GE.1.AND.I.GT.1)GO TO 70
      BF(I)=BJ
   10 AL=AL+DAL
```

```
C
 1005 CONTINUE
C.....BEGIN FREQUENCY LOOP
      FR = FRCN(1)
      FRMAX = FRCN(2)
      FRINC = 10.**FRCN(3)
      II=0
 1010 CONTINUE
      II=II+1
C
      F=FR*1.E+6
      W=TP*F
C
C.....RESULTANT PROPAGATION CONSTANT, GAMMA, FOR EACH LAYER AT THIS
C     FREQUENCY.....
      DO 12 M = 1,MC
      EMU = EMUR(M)*EMUO
      EPS = EPSR(M)*EPSO
      SIG = SIGR(M)*SIGC
      GMR = - W*W*EMU*EPS
      GMI = W*EMU*SIG
   12 GS(M)=CMPLX(GMR,GMI)
C
C.....INTEGRATION LOOP
      AL=0.
      SUMD=0.
      HT(MC)=0.
      SZR(MC) = 1.
      DO 50 I=1,IMAX
      ALS=AL*AL
      DO 14 M = 1,MC
   14 TAU(M) = CSQRT(ALS + GS(M))
C
C.....HYPERBOLIC FUNCTION CALCS
      DO 18 M=2,MCM
      PSY(M)=TAU(M)*D(M)
      CEP = CEXP(PSY(M))
      CEM = 1./CEP
      CSPL(M)=(CEP+CEM)/2.
      HT (M) = (CEP-CEM)/(CEP+CEM)
   18 CONTINUE
C
C.....CALCULATE IMPEDENCE RATIOS.....
      DO 32 MR = 1, MCM
      M = MCM-MR + 1
      MP = M+1
   32 SZR(M) = (TAU(M)/TAU(MP))*(SZR(MP)+HT(MP))/(1.+SZR(MP)*HT(MP))
     1     *(EMUR(MP)/EMUR(M))
C
C.....CALCULATE ALL POSSIBLE POLES
      POLE(1) = 1. + SZR(1)
      PROD = 2./POLE(1)
      DO 34 M = 2, MCM
      POLE(M) = 1. + SZR(M)*HT(M)
```

```
   34 PROD = PROD/(POLE(M)*CSPL(M))
      TRAN(I) = PROD
      ZMAG=CABS(SZR(2))
      ZREAL=REAL(SZR(2))
      ZIM=AIMAG(SZR(2))
      ZPHA=ATAN2(ZIM,ZREAL)
  500 FORMAT(/,2X,*SPACING=*,F8.5,5X,*MAG=*,E14.7,5X,*PHASE=*,E14.7)
C     REFL(I) = (SZR(1)-1.)/(SZR(1)+1.)
      TZMD = TAU(1)*ZMD
      CE=CEXP(-TZMD)
      FACT = ALS*TRAN(I)*CE*BF(I)/TAU(1)
   40 SUMD = SUMD + FACT
C.....DEBUG PRINTOUT.....
      IF(IDBP.EQ.0)GO TO 42
      IF(MOD(I,100).NE.0)GO TO 42
      WRITE(6,114)(GS(M),TAU(M),PSY(M),HT(M),M=1,MC)
      WRITE(6,115)(CSPL(M),SZR(M),POLE(M),M=1,MC)
      WRITE(6,116)ALS,PROD,CE,BF(I)
      WRITE(6,117)FACT,SUMD
   42 CONTINUE
      AL=AL+DAL
  789 CONTINUE
   50 CONTINUE
C     .....END OF INTEGRATION LOOP.....
C
   51 CONTINUE
      SUMD=SUMD*DAL
      CSUMD=CABS(SUMD)
      SHEF(II)=9999.
      IF(CSUMD.GE.1.E-40)SHEF(II)=-20.*ALOG10(TERM*CSUMD)
      SH(II,KK)=SHEF(II)
      FREQ(II)=F
      FLOG(II)=ALOG10(FR)
      FR=FR*FRINC
      IF(FR.LE.FRMAX)GO TO 1010
C.....END OF FREQUENCY LOOP
C
      WRITE(6,104)
      WRITE(6,105)(FREQ(I),SHEF(I),I=1,II)
      WRITE(6,106)
      IF(NGO.EQ.1)GO TO 1000
C
C.....PRINTER PLOT
      IF(IPLT.LE.0)GO TO 66
      BCD(1)=10HSHIELDING
      BCD(2)=10HEFFECTIVEN
      BCD(3)=10HESS
      CALL STPLT2(1,FLOG,SHEF,II)
      CALL PLOT1(0,2,20,8,10)
      CALL PLOT2(IMAGE,2.,-5.,200.,0.)
      CALL PLOT3(1H.,FLOG,SHEF,II,IMAGE)
      CALL PLOT4(28,BCD,IMAGE)
      WRITE(6,107)
```

```
C
C.....END OF PROBLEM LOOP
C
C
C.....DRUM PLOT
      CALL COMPRS
      CALL BGNPL(0)
      DO 65 K=1,KK
      DO 61 I=1,II
   61 SHEF(I)=SH(I,K)
      IF(K.GT.1)GO TO 62
      SH1=100.
      SH2=1.3
      SV1=0.
      SV2=40.
      DO 60 I=1,7
   60 LX(I)=LY(I)=LM(I)=10H
      LX(3)=10HFREQUENCY
      LX(4)=10H(HZ)
      LY(2)=10HSHIELDING
      LY(3)=10HEFFECTIVEN
      LY(4)=10HESS (DB)
      CALL TITLE(LL,-70,LX,70,LY,40,8.,5.)
      CALL XLOG(SH1,SH2,SV1,SV2)
   62 CALL CURVE(FREQ,SHEF,II,12)
   65 CONTINUE
      CALL ENDPL(KK)
      CALL DONEPL
   66 CONTINUE
C
      GO TO 71
   70 WRITE(6,112) IERROR
      STOP 10
   71 CONTINUE
  100 FORMAT(1H1,/////,30X,*PROBLEM *,I2,* INPUT DATA*,//)
  101 FORMAT(20X,*FREQUENCY = *,E13.6,* HZ*,10X,*LAMDA = *,E13.6)
  102 FORMAT(   5(5X,2E10.3))
  104 FORMAT(1H1,30X,*FREQ(HZ)*,10X,*SHEF(DB)*,//)
  105 FORMAT(30X,E10.3,5X,F10.3)
  106 FORMAT(1H1)
  107 FORMAT(30X,*FREQUENCY (MHZ) EXPONENT  *,1H1)
  109 FORMAT(25X,2E13.6,5X,E13.6,5X,2E13.6)
  110 FORMAT(//)
  111 FORMAT(//,20X,*DENOMINATOR TOO SMALL FOR F=*,E13.6,* HZ*,//)
  112 FORMAT(10X,*BESSEL FUNCTION ERROR, IER = *,I4)
  114 FORMAT(4(4X,2E13.6))
  115 FORMAT(3(2X,2E13.6))
  116 FORMAT(/,5X,E13.6,2(5X,2E13.6),5X,E13.6)
  117 FORMAT(/,25X,2(10X,2E13.6))
      END
      SUBROUTINE IADATA
      COMMON/PARAMS/NOPT(7),T(7),SIGR(7),EMUR(7),EPSR(7),DLUP(7),FRCN(7)
     1,NGO,LL(7)
```

```
C
      NGO=0
      WRITE(6,501)
      READ(5,601)NOPT(1)
      MC=NOPT(1)
      T(1)=T(MC)=.305
      DO 5 IU=1,MC
      EPSR(IU)=1.
      EMUR(IU)=1.
    5 CONTINUE
      NOPT(2)=1000
      NOPT(3)=0
      NOPT(4)=0
      DLUP(1)=.152
      DLUP(2)=.1
      SIGR(1)=SIGR(MC)=0.
      MCM=MC-1
      DO 10 IKI=2,MCM
      WRITE(6,502)IKI
      READ(5,602)T(IKI)
      WRITE(6,503)IKI
      READ(5,603)SIGR(IKI)
   10 CONTINUE
      WRITE(6,504)
      READ(5,604)FRCN(1)
      WRITE(6,505)
      READ(5,605)FRCN(2)
      FRCN(3)=.125
      WRITE(6,506)
      READ(5,601)NGO
  501 FORMAT(/,2X,*ENTER NO. OF LAYERS*)
  502 FORMAT(/,2X,*ENTER THICKNESS OF LAYER*,2X,I2)
  503 FORMAT(/,2X,*ENTER SIGR OF LAYER*,2X,I2)
  504 FORMAT(/,2X,*ENTER START FREQ.*)
  505 FORMAT(/,2X,*ENTER MAX FREQ.*)
  506 FORMAT(/,2X,*MORE DATA LATER? Y=1,N=0*)
  601 FORMAT(I2)
  602 FORMAT(F14.8)
  603 FORMAT(F14.8)
  604 FORMAT(F14.8)
  605 FORMAT(F14.8)
      RETURN
      END
      SUBROUTINE BESJ(X,N,BJ,D,IER)
C
      BJ=.0
      IF(N)10,20,20
   10 IER=1
      RETURN
   20 IF(X)30,30,31
   30 IER=2
      RETURN
   31 IF(X-15.)32,32,34
   32 NTEST=20.+10.*X-X**2/3
      GO TO 36
```

```
   34 NTEST=90.+X/2.
   36 IF(N-NTEST)40,38,38
   38 IER=4
      RETURN
   40 IER=0
      N1=N+1
      BPREV=.0
C
C     COMPUTE STARTING VALUE OF M
C
      IF(X-5.)50,60,60
   50 MA=X+6.
      GO TO 70
   60 MA=1.4*X+60./X
   70 MB=N+IFIX(X)/4+2
      MZERO=MAX0(MA,MB)
C
C     SET UPPER LIMIT OF M
C
      MMAX=NTEST
  100 DO 190 M=MZERO,MMAX,3
C
C     SET F(M),F(M-1)
C
      FM1=1.0E-28
      FM=.0
      ALPHA=.0
      IF(M-(M/2)*2)120,110,120
  110 JT=-1
      GO TO 130
  120 JT=1
  130 M2=M-2
      DO 160 K=1,M2
      MK=M-K
      BMK=2.*FLOAT(MK)*FM1/X-FM
      FM=FM1
      FM1=BMK
      IF(MK-N-1)150,140,150
  140 BJ=BMK
  150 JT=-JT
      S=1+JT
  160 ALPHA=ALPHA+BMK*S
      BMK=2.*FM1/X-FM
      IF(N)180,170,180
  170 BJ=BMK
  180 ALPHA=ALPHA+BMK
      BJ=BJ/ALPHA
      IF(ABS(BJ-BPREV)-ABS(D*BJ))200,200,190
  190 BPREV=BJ
      IER=3
  200 RETURN
      END
C>
```

```
      PROGRAM APRAD (INPUT,OUTPUT,TAPE5=INPUT,TAPE6=OUTPUT)
      DIMENSION RCXP(7),RCYP(7)
      DIMENSION DXDY(9,17)
      DIMENSION EPHIR(5,9),EPHII(5,9)
      DIMENSION EXR(9,17),EXI(9,17),EYR(9,17),EYI(9,17)
      DIMENSION RREC(7),RFR(7)
      DIMENSION SHEFA(100),FREQA(100)
      REAL HZFRR,HZFRI
      REAL MCXR(9,17),MCXI(9,17),MCYR(9,17),MCYI(9,17)
      REAL MAG
      REAL HTHR,HTHI
      COMPLEX TRAN
      COMPLEX TRANFR(9,17)
      COMPLEX MX,MY,CEP,FXI,FYI,BARG
      COMPLEX MCX,MCY,CHZX,CHZY,HZ
      COMPLEX FLUX,HZF(7),HZA(7)
      DIMENSION WEIT(7)
      REAL MUO
      COMPLEX ZHAT
      REAL LAM
      COMMON/BLOCK1/W,F
      COMMON/PARAMS/NOPT(7),T(7),SIGR(7),EMUR(7),EPSR(7),DLUP(7),
     +FRCN(7),NGO,LL(7)
      DATA RFR/.6096,.7620,.9144,1.0668,1.2192,
     +1.8288,2.4384/
      DATA RREC/.3048,.4572,.6096,.7620,.9144,
     +1.5240,2.1336/
      DATA WEIT/.25,.125,.125,.125,.125,.125,.125/
C  RCXP AND RCYP ARE THE POINTS FOR INTEGRATION OVER THE
C  RECEIVING 12 IN. LOOPS
      DATA RCXP/0.0,.06205374,.12410748,.06205374,-.06205374,
     +-.12410748,-.06205374/
      DATA RCYP/0.0,.107480231,0.0,-.107480231,-.107480231,0.0,
     +.107480231/
      PI=3.1415926536
      TP=2.*PI
      PIOT=PI/2.
      ETA=377.
      MUO=4.*PI*1.E-07
      DO 5 I=1,9
      DO 5 J=1,17
      TRANFR(I,J)=(1.0,0.0)
    5 CONTINUE
C  A IS THE AREA OF THE LOOP ANTENNAS
      A=7.258335668E-2
C  PROBLEM LOOP
      KKK=0
 1000 CONTINUE
      KKK=KKK+1
      WRITE (6,400)KKK
      CALL IADATA
      FR=FRCN(1)
      FRMAX=FRCN(2)
      FRINC=10.**FRCN(3)
      IFLP=0
```

```
 1234 F=FR*1.E+6
      IFLP=IFLP+1
      FREQA(IFLP)=F
      W=TP*F
      LAM=(3.0E08)/F
      IMAX=NOPT(1)
      JMAX=NOPT(2)
      DX=DLUP(1)/FLOAT(IMAX-1)
      DY=DLUP(2)/FLOAT(JMAX-1)
      IMAX21=IMAX/2+1
      IMAX22=IMAX/2+2
      JMAX21=JMAX/2+1
      JMAX22=JMAX/2+2
C
C  DIFFERENTIAL AREA ASSIGNMENT
C
      DO 25 I=1,IMAX
      DO 25 J=1,JMAX
      IF(I .NE. IMAX21 .AND. I .NE. IMAX22) GO TO 26
      IF(I .EQ. IMAX21 .OR. I .EQ. IMAX22) GO TO 27
   26 IF(J .EQ. JMAX21 .OR. J .EQ. JMAX22) GO TO 28
      DXDY(I,J)=DX*DY
      GO TO 25
   28 DXDY(I,J)=(DX*DY)/2.
      GO TO 25
   27 IF(J .EQ. JMAX21 .OR. J .EQ. JMAX22) GO TO 29
      DXDY(I,J)=(DX*DY)/2.
      GO TO 25
   29 DXDY(I,J)=(DX*DY)/4.
   25 CONTINUE
C
C  RFR IS THE ANTENNA SEPARATION IN FREE SPACE
C  RREC IS THE DISTANCE OF THE RECEIVING ANTENNA FROM THE APERTURE
C
C
C  CALCULATE FREE SPACE FLUX THROUGH ANTENNA
C
      DO 20 I=1,1
      DO 10 J=1,7
      X=RCXP(J)
      Y=RCYP(J)
      XYS=SQRT(X*X+Y*Y)
      XYZS=SQRT(X*X+Y*Y+RFR(I)**2)
      DEL=SQRT(X*X+Y*Y)
      ARG=DEL/RFR(I)
      THETA=ATAN(ARG)
      FFRE=A*COS(THETA)/TP
      R=RFR(I)/COS(THETA)
      BETA=TP/LAM
      BETR=BETA*R
      HTHR=((-1.)*(BETA**2)*SIN(THETA)*A/(4.*PI*R))*(COS(BETR)
     +-SIN(BETR)/(BETR)-COS(BETR)/(BETR**2))
      HTHI=((-1.)*(BETA**2)*SIN(THETA)*A/(4.*PI*R))*(SIN(BETR)/(BETR
     +**2)-SIN(BETR)-COS(BETR)/(BETR))
      HZFRR=FFRE*(COS(BETR)/(R**3)+BETA*SIN(BETR)/(R**2))*COS(THETA)
      HZFRI=FFRE*(BETA*COS(BETR)/(R**2)-SIN(BETR)/(R**3))*COS(THETA)
```

```
 10   HZF(J)=CMPLX((HZFRR*RFR(I)/XYZS)-(HTHR*XYS/XYZS),
     +(HZFRI*RFR(I)/XYZS)-(HTHI*XYS/XYZS))
      FLUX=(0.0,0.0)
      DO 15 II=1,7
 15   FLUX=FLUX+A*WEIT(II)*HZF(II)
      MAG=CABS(FLUX)
      DB=20.*ALOG10(MAG)
 20   DB1=DB
C
C  START TAN E FIELD LOOP (FIRST QUAD. ONLY)
C
 445  CONTINUE
      DO 50 I=1,IMAX21
      DO 50 J=1,JMAX21
      X=(I-1)*DX
      Y=(J-1)*DY
      DEL=SQRT(X*X+Y*Y)
      ARG=DEL/(.305)
      THETA=ATAN(ARG)
      COTHE=COS(THETA)
      SITHE=SIN(THETA)
      R=(.305)/COTHE
      BETR=(TP*R)/LAM
      COSBR=COS(BETR)
      SINBR=SIN(BETR)
      FACT=(ETA*PI*A*SITHE)/(LAM*LAM*R)
      EPHIR(I,J)=FACT*(COSBR-(SINBR/BETR))
      EPHII(I,J)=(-1.)*FACT*(SINBR+(COSBR/BETR))
      IF(EPHIR(I,J) .LT. 1.0E-05) EPHIR(I,J)=0.0
      IF(I.EQ.1)GO TO 40
      PHI=ATAN(Y/X)
 40   IF(I.EQ.1)PHI=PIOT
      IF(NOPT(4) .EQ. 0) GO TO 456
      U=(TP/LAM)*SITHE*COS(PHI)
      V=(TP/LAM)*SITHE*SIN(PHI)
      CALL SHIELD(U,V,R,TRAN)
      TRANFR(I,J)=TRAN
 510  FORMAT(/,2X,*TRAN=*,2E14.7)
 456  CONTINUE
      EXR(I,J)=EPHIR(I,J)*SIN(PHI)
      EXI(I,J)=EPHII(I,J)*SIN(PHI)
      EYR(I,J)=EPHIR(I,J)*COS(PHI)
      EYI(I,J)=EPHII(I,J)*COS(PHI)
      IF(I .EQ. 1) EYR(I,J)=EYI(I,J)=0.0
 50   CONTINUE
C
 701  FORMAT(/,2X,*FLAG1*)
C  END TAN E FIELD LOOP
C
C  FILL UP OTHER QUADRANTS
C
      DO 1 J=1,JMAX21
      DO 1 I=2,IMAX21
      II=IMAX-(I-2)
      TRANFR(II,J)=TRANFR(I,J)
      EXR(II,J)=EXR(I,J)
      EXI(II,J)=EXI(I,J)
      EYR(II,J)=EYR(I,J)
```

```
  1    EYI(II,J)=EYI(I,J)
       DO 2 I=1,IMAX21
       DO 2 J=2,JMAX21
       JJ=JMAX-(J-2)
       TRANFR(I,JJ)=TRANFR(I,J)
       EXR(I,JJ)=EXR(I,J)
       EXI(I,JJ)=EXI(I,J)
       EYR(I,JJ)=EYR(I,J)
  2    EYI(I,JJ)=EYI(I,J)
       DO 3 I=2,IMAX21
       DO 3 J=2,JMAX21
       II=IMAX21+I
       JJ=JMAX21+J
       TRANFR(II,JJ)=TRANFR(I,J)
       EXR(II,JJ)=EXR(I,J)
       EXI(II,JJ)=EXI(I,J)
       EYR(II,JJ)=EYR(I,J)
  3    EYI(II,JJ)=EYI(I,J)
C
C  CORRECT SIGNS OF X & Y COMPONENTS
C
       DO 60 I=1,IMAX
       DO 60 J=1,JMAX
       IF(I .LT. IMAX22 .AND. J .LT. JMAX22) GO TO 61
       IF(I .LT. IMAX22 .AND. J .GE. JMAX22) GO TO 60
       IF(I .GE. IMAX22 .AND. J .LT. JMAX22) GO TO 62
       IF(I .GE. IMAX22 .AND. J .GE. JMAX22) GO TO 63
 61    EXR(I,J)=(-1.)*EXR(I,J)
       EXI(I,J)=(-1.)*EXI(I,J)
       GO TO 60
 62    EXR(I,J)=(-1.)*EXR(I,J)
       EXI(I,J)=(-1.)*EXI(I,J)
       EYR(I,J)=(-1.)*EYR(I,J)
       EYI(I,J)=(-1.)*EYI(I,J)
       GO TO 60
 63    EYR(I,J)=(-1.)*EYR(I,J)
       EYI(I,J)=(-1.)*EYI(I,J)
   60 CONTINUE
C
C  CALCULATE MAGNETIC CURRENT
C
       DO 70 I=1,IMAX
       DO 70 J=1,JMAX
       MCXR(I,J)=2.*EYR(I,J)
       MCXI(I,J)=2.*EYI(I,J)
       MCYR(I,J)=(-2.)*EXR(I,J)
       MCYI(I,J)=(-2.)*EXI(I,J)
   70 CONTINUE
C
```

```
C  CALCULATE Z COMPONENT OF H FIELD AT POINT XPP,YPP IN RECEIVER PLANE
C
      DO 80 K=1,1
      DO 90 IR=1,7
      XPP=RCXP(IR)
      YPP=RCYP(IR)
      HZA(IR)=CMPLX(0.0,0.0)
      DO 30 I=1,IMAX
      DO 30 J=1,JMAX
C
C  APERTURE COORDINATES
C
      IF(I .LT. IMAX22 .AND. J .LT. JMAX22) GO TO 31
      IF(I .LT. IMAX22 .AND. J .GE. JMAX22) GO TO 32
      IF(I .GE. IMAX22 .AND. J .GE. JMAX22) GO TO 33
      IF(I .GE. IMAX22 .AND. J .LT. JMAX22) GO TO 34
   31 XP=(I-1)*DX
      YP=(J-1)*DY
      GO TO 35
   32 XP=(I-1)*DX
      YP=(-1.)*(JMAX-J+1)*DY
      GO TO 35
   33 XP=(-1.)*(IMAX-I+1)*DX
      YP=(-1.)*(JMAX-J+1)*DY
      GO TO 35
   34 XP=(-1.)*(IMAX-I+1)*DX
      YP=(J-1)*DY
   35 RMRP=SQRT((XP-XPP)**2+(YP-YPP)**2+RREC(K)**2)
      DENOM=RMRP**5
      TK=(TP/LAM)*RMRP*(-1.0)
      BARG=CMPLX(0.0,TK)
      CEP=CEXP(BARG)
      MCX=CMPLX(MCXR(I,J),MCXI(I,J))*TRANFR(I,J)
      MCY=CMPLX(MCYR(I,J),MCYI(I,J))*TRANFR(I,J)
C
C  CHZX IS THE CONTRIBUTION TO HZ FROM MCX (X COMP. OF MAG. CURRENT)
C  CHZY IS THE CONTRIBUTION TO HZ FROM MCY (Y COMP. OF MAG. CURRENT)
C
      CHZY=3.*(YPP-YP)*RREC(K)*MCY*CEP*DXDY(I,J)/(DENOM*4.*PI)
      CHZX=3.*(XPP-XP)*RREC(K)*MCX*CEP*DXDY(I,J)/(DENOM*4.*PI)
      ZHAT=CMPLX(0.0,(-1.)/(W*MUO))
      CHZX=CHZX*ZHAT
      CHZY=CHZY*ZHAT
   30 HZA(IR)=HZA(IR)+CHZX+CHZY
   90 CONTINUE
      FLUX=(0.0,0.0)
      DO 95 JI=1,7
   95 FLUX=FLUX+A*WEIT(JI)*HZA(JI)
      MAG=CABS(FLUX)
      DB=20.*ALOG10(MAG)
```

```
 80   DB2=DB
      SHEF=DB1-DB2
      SHEFA(IFLP)=SHEF
      FR=FR*FRINC
      IF(FR .LE. FRMAX) GO TO 1234
      WRITE(6,104)
      WRITE(6,105)(FREQA(I),SHEFA(I),I=1,IFLP)
444   CONTINUE
      IF (NGO .EQ. 1) GO TO 1000
100   FORMAT(/,15X,*X COMPONENT*)
200   FORMAT(/,15X,*Y COMPONENT*)
209   FORMAT(/,2X,*POINT*,F5.2,1X,F5.2)
210   FORMAT(/,2X,*DISTANCE=*,F7.4,2X,*HZ=*,2E14.6)
300   FORMAT(/,2X,*PHI COMPONENT*)
301   FORMAT(/,2X,*I*,3X,*J*.3X,*DEL*,5X,*THETA*)
302   FORMAT(/,2X,I2,3X,I2,3X,F7.4,5X,F7.4)
 303  FORMAT(/,2X,*PHI COMP. INSIDE LOOP*)
 304  FORMAT(/,2X,I2,3X,I2,3X,E14.7,2X,E14.7)
 305  FORMAT(/,2X,I2,3X,I2,3X,*PHI=*,F8.4,*PI*)
306   FORMAT(/,3X,*MAG. CURRENT*)
307   FORMAT(/,3X,*I*,3X,*J*,3X,*MCXR*,14X,*MCXI*,14X,*MCYR*,14X,*MCYI*)
308   FORMAT(/,3X,I2,3X,I2,4(E14.7))
309   FORMAT(/,3X,I2,3X,I2,4(E14.7))
310   FORMAT(/,3X,*I*,3X,*J*,3X,*EXR*,14X,*EXI*,14X,*EYR*,14X,*EYI*)
311   FORMAT(/,2X,*FREE SPACE*)
312   FORMAT(/,2X,*APERTURE*)
313   FORMAT(/,2X,*DISTANCE=*,F7.4,2X,*HZFR=*,2E14.6)
314   FORMAT(/,2X,*DISTANCE=*,F7.4,2X,*FLUX=*,2E14.6,2X,*DB=*,F10.4)
400   FORMAT(1H1,/////,30X,*PROBLEM *,I2,* INPUT DATA *,//)
500   FORMAT(/,2X,*HELP*)
501   FORMAT(/,2X,*HELP1*)
104   FORMAT(1H1,30X,*FREQ(HZ)*,10X,*SHEF(DB)*,//)
105   FORMAT(30X,E10.3,5X,F10.3)
999   CONTINUE
      STOP
      END
      SUBROUTINE SHIELD(U,V,R,TRAN)
      COMMON/BLOCK1/W,F
      COMMON/PARAMS/NOPT(7),T(7),SIGR(7),EMUR(7),EPSR(7),
     +DLUP(7),FRCN(7),NGO,LL(7)
      COMPLEX CEP,CEN
      COMPLEX TOP,BOT
      COMPLEX TRAN,PROD
      COMPLEX GS(7),TAU(7),PSY(7),HT(7),SZR(7),POLE(7),CSPL(7)
      COMPLEX Z(7)
      REAL LAM
      PI=3.1415926536
      EMU0=1.26E-6
      EPS0=8.854E-12
      SIGC=5.80E+7
      LAM=(3.0E08)/F
      R0=R
```

```
C....MC IS THE TOTAL NO. OF LAYERS
      MC=NOPT(3)
      MCM=MC-1
C....CALCULATE LAYER IMPEDANCES
      DO 5 M=1,MC
      EMU=EMUR(M)*EMUO
      EPS=EPSR(M)*EPSO
      SIG=SIGR(M)*SIGC
      IF(SIGR(M) .NE. 0.0) GO TO 6
      BETA=(2.*PI)/LAM
      IF(MC .EQ. 5 .AND. M .EQ. 3)R=RO+T(2)+T(3)
      IF(MC .EQ. 5 .AND. M .EQ. 5)R=RO+T(2)+T(3)+T(4)
      IF(MC .EQ. 7 .AND. M .EQ. 3)R=RO+T(2)+T(3)
      IF(MC .EQ. 7 .AND. M .EQ. 5)R=RO+T(2)+T(3)+T(4)+T(5)
      IF(MC .EQ. 7 .AND. M .EQ. 7)R=RO+T(2)+T(3)+T(4)+T(5)+T(6)
      TOP=CMPLX((-1.0)*(BETA**2)*(R**2),BETA*R)
      BOT=CMPLX(1.-(BETA**2)*(R**2),BETA*R)
      Z(M)=(377.)*(TOP/BOT)
 100  FORMAT(/,2X,I2,5X,2E14.6)
      GO TO 5
   6  SKDP=(1.0)/(SQRT(PI*F*EMU*SIG))
      Z(M)=CMPLX(1./(SIG*SKDP),1./(SIG*SKDP))
   5  CONTINUE
      DO 10 M=1,MC
      EMU=EMUR(M)*EMUO
      EPS=EPSR(M)*EPSO
      SIG=SIGR(M)*SIGC
      GMR=-W*W*EMU*EPS
      GMI=W*EMU*SIG
  10  GS(M)=CMPLX(GMR,GMI)
      AL=SQRT(U*U+V*V)
      HT(MC)=0.
      SZR(MC)=1.
      DO 11 M=1,MC
  11  TAU(M)=CSQRT(GS(M)+U*U+V*V)
      DO 12 M=2,MCM
      PSY(M)=TAU(M)*T(M)
      CEP=CEXP(PSY(M))
      CEM=1./CEP
      CSPL(M)=(CEP+CEM)/2.
      HT(M)=(CEP-CEM)/(CEP+CEM)
  12  CONTINUE
      DO 13 MR=1,MCM
      M=MCM-MR+1
      MP=M+1
  13  SZR(M)=(Z(MP)/Z(M))*(SZR(MP)+HT(MP))/(1.+SZR(MP)*HT(MP))
      POLE(1)=1.+SZR(1)
      PROD=2.*(Z(MC)/Z(1))/POLE(1)
      DO 14 M=2,MCM
      POLE(M)=1.+SZR(M)*HT(M)
  14  PROD=PROD/(POLE(M)*CSPL(M))
      TRAN=PROD
      RETURN
      END
      SUBROUTINE IADATA
      COMMON/PARAMS/NOPT(7),T(7),SIGR(7),EMUR(7),EPSR(7),DLUP(7),FRCN(7)
     1,NGO,LL(7)
```

```
      NGO=0
      WRITE (6,600)
      READ (5,500)FRCN(1)
      WRITE(6,607)
      READ(5,500)FRCN(2)
      FRCN(3)=.125
      WRITE (6,601)
      READ (5,501)DLUP(1)
      WRITE (6,651)
      READ (5,501)DLUP(2)
      WRITE (6,602)
      READ (5,502)NOPT(1)
      WRITE (6,652)
      READ (5,502)NOPT(2)
      WRITE (6,603)
      READ (5,503)NOPT(4)
      IF(NOPT(4) .EQ. 0) GO TO 30
      WRITE (6,604)
      READ (5,504)NOPT(3)
      MC=NOPT(3)
      MCM=MC-1
      DO 10 I=2,MCM
      WRITE (6,605)I
      READ (5,505)T(I)
      READ (5,505)SIGR(I)
   10 CONTINUE
   30 CONTINUE
      T(1)=T(MC)=.305
      SIGR(1)=SIGR(MC)=0.0
      WRITE (6,606)
      READ (5,506)NGO
      DO 20 I=1,MC
      EMUR(I)=1.0
   20 EPSR(I)=1.0
  600 FORMAT(/,2X,*ENTER START FREQ (MHZ)*)
  601 FORMAT(/,2X,*APERTURE HEIGHT*)
  651 FORMAT(/,2X,*APERTURE WIDTH*)
  602 FORMAT(/,2X,*X POINTS*)
  652 FORMAT(/,2X,*Y POINTS*)
  603 FORMAT(/,2X,*SHIELDING MATERIAL IN APERTURE? Y=1,N=0*)
  604 FORMAT(/,2X,*HOW MANY LAYERS? (TYRAS M+1)*)
  605 FORMAT(/,2X,*ENTER THICKNESS AND SIGR OF LAYER NO.*,1X,I2)
  606 FORMAT(/,2X,*MORE DATA LATER? Y=1, N=0*)
  607 FORMAT(/,2X,*MAX FREQ (MHZ)*)
  500 FORMAT(E10.1)
  501 FORMAT(2E10.1)
  502 FORMAT(I2)
  503 FORMAT(I2)
  504 FORMAT(I2)
  505 FORMAT(F14.8)
  506 FORMAT(I2)
      RETURN
      END
```

Chief of Engineers
ATTN: Tech Monitor
ATTN: DAEN-ASI-L (2)
ATTN: DAEN-CCP
ATTN: DAEN-CW
ATTN: DAEN-CWE
ATTN: DAEN-CWM-R
ATTN: DAEN-CWO
ATTN: DAEN-CWP
ATTN: DAEN-MP
ATTN: DAEN-MPC
ATTN: DAEN-MPE
ATTN: DAEN-MPO
ATTN: DAEN-MPR-A
ATTN: DAEN-RD
ATTN: DAEN-RDC
ATTN: DAEN-RDM
ATTN: DAEN-RM
ATTN: DAEN-ZC
ATTN: DAEN-ZCE
ATTN: DAEN-ZCI
ATTN: DAEN-ZCM

FESA, ATTN: Library 22060

US Army Engineer Districts
ATTN: Library
Alaska 99501
Al Batin 09616
Albuquerque 87103
Baltimore 21203
Buffalo 14207
Charleston 29402
Chicago 60604
Detroit 48231
Far East 96301
Fort Worth 76102
Galveston 77550
Huntington 25721
Jacksonville 32232
Japan 96343
Kansas City 64106
Little Rock 72203
Los Angeles 90053
Louisville 40201
Memphis 38103
Mobile 36628
Nashville 37202
New Orleans 70160
New York 10007
Norfolk 23510
Omaha 68102
Philadelphia 19106
Pittsburgh 15222
Portland 97208
Riyadh 09038
Rock Island 61201
Sacramento 95814
San Francisco 94105
Savannah 31402
Seattle 98124
St. Louis 63101
St. Paul 55101
Tulsa 74102
Vicksburg 39180
Walla Walla 99362
Wilmington 28401

US Army Engineer Divisions
ATTN: Library
Europe 09757
Huntsville 35807
Lower Mississippi Valley 39180
Middle East 09038
Middle East (Rear) 22601
Missouri River 68101
New England 02154
North Atlantic 10007
North Central 60605
North Pacific 97208
Ohio River 45201
Pacific Ocean 96858
South Atlantic 30303
South Pacific 94111
Southwestern 75202

US Army Europe
HQ, 7th Army Training Command 09114
ATTN: AETTG-DEH (5)
HQ, 7th Army ODCS/Engr. 09403
ATTN: AEAEN-EH (4)
V. Corps 09079
ATTN: AETVDEH (5)
VII. Corps 09154
ATTN: AETSDEH (5)
21st Support Command 09325
ATTN: AEREH (5)
Berlin 09742
ATTN: AEBA-EN (2)
Southern European Task Force 09168
ATTN: AESE-ENG (3)
Installation Support Activity 09403
ATTN: AEUES-RP

8th USA, Korea
ATTN: EAFE (8) 96301
ATTN: EAFE-Y 96358
ATTN: EAFE-ID 96224
ATTN: EAFE-AM 96208
ATTN: EAFE-H 96271
ATTN: EAFE-P 96259
ATTN: EAFE-T 96212

416th Engineer Command 60623
ATTN: Facilities Engineer

USA Japan (USARJ)
Ch, FE Div, AJEN-FE 96343
Fac Engr (Honshu) 96343
Fac Engr (Okinawa) 96331

ROK/US Combined Forces Command 96301
ATTN: EUSA-HHC-CFC/Engr

US Military Academy 10996
ATTN: Facilities Engineer
ATTN: Dept of Geography & Computer Science
ATTN: DSCPER/MAEN-A

Engr. Studies Center 20315
ATTN: Library

AMMRC, ATTN: DRXMR-WE 02172

USA ARRCOM 61299
ATTN: DRCIS-RI-I
ATTN: DRSAR-IS

DARCOM - Dir., Inst., & Svcs.
ATTN: Facilities Engineer
ARRADCOM 07801
Aberdeen Proving Ground 21005
Army Matls. and Mechanics Res. Ctr.
Corpus Christi Army Depot 78419
Harry Diamond Laboratories 20783
Dugway Proving Ground 84022
Jefferson Proving Ground 47250
Fort Monmouth 07703
Letterkenny Army Depot 17201
Natick R&D Ctr. 01760
New Cumberland Army Depot 17070
Pueblo Army Depot 81001
Red River Army Depot 75501
Redstone Arsenal 35809
Rock Island Arsenal 61299
Savanna Army Depot 61074
Sharpe Army Depot 95331
Seneca Army Depot 14541
Tobyhanna Army Depot 18466
Tooele Army Depot 84074
Watervliet Arsenal 12189
Yuma Proving Ground 85364
White Sands Missile Range 88002

DLA ATTN: DLA-WI 22314

FORSCOM
FORSCOM Engineer, ATTN: AFEN-FE
ATTN: Facilities Engineer
Fort Buchanan 00934
Fort Bragg 28307
Fort Campbell 42223
Fort Carson 80913
Fort Devens 01433
Fort Drum 13601
Fort Hood 76544
Fort Indiantown Gap 17003
Fort Irwin 92311
Fort Sam Houston 78234
Fort Lewis 98433
Fort McCoy 54656
Fort McPherson 30330
Fort George G. Meade 20755
Fort Ord 93941
Fort Polk 71459
Fort Richardson 99505
Fort Riley 66442
Presidio of San Francisco 94129
Fort Sheridan 60037
Fort Stewart 31313
Fort Wainwright 99703
Vancouver Bks. 98660

HSC
ATTN: HSLO-F 78234
ATTN: Facilities Engineer
Fitzsimons Army Medical Center 80240
Walter Reed Army Medical Center 20012

INSCOM - Ch, Instl. Div.
ATTN: Facilities Engineer
Arlington Hall Station (2) 22212
Vint Hill Farms Station 22186

MDW
ATTN: Facilities Engineer
Cameron Station 22314
Fort Lesley J. McNair 20319
Fort Myer 22211

MTMC
ATTN: MTMC-SA 20315
ATTN: Facilities Engineer
Oakland Army Base 94626
Bayonne MOT 07002
Sunny Point MOT 28461

NARADCOM, ATTN: DRDNA-F 01760

TARCOM, Fac. Div. 48090

TECOM, ATTN: DRSTE-LG-F 21005

TRADOC
HQ, TRADOC, ATTN: ATEN-FE
ATTN: Facilities Engineer
Fort Belvoir 22060
Fort Benning 31905
Fort Bliss 79916
Carlisle Barracks 17013
Fort Chaffee 72902
Fort Dix 08640
Fort Eustis 23604
Fort Gordon 30905
Fort Hamilton 11252
Fort Benjamin Harrison 46216
Fort Jackson 29207
Fort Knox 40121
Fort Leavenworth 66027
Fort Lee 23801
Fort McClellan 36205
Fort Monroe 23651
Fort Rucker 36362
Fort Sill 73503
Fort Leonard Wood 65473

TSARCOM, ATTN: STSAS-F 63120

USACC
ATTN: Facilities Engineer
Fort Huachuca 85613
Fort Ritchie 21719

WESTCOM
ATTN: Facilities Engineer
Fort Shafter 96858

SHAPE 09055
ATTN: Survivability Section, CCB-OPS
Infrastructure Branch, LANMA

HQ USEUCOM 09128
ATTN: ECJ 4/7-LOE

Fort Belvoir, VA 22060
ATTN: ATZA-DTE-EM
ATTN: ATZA-DTE-SM
ATTN: ATZA-FE
ATTN: Engr. Library
ATTN: Canadian Liaison Office (2)
ATTN: IWR Library

Cold Regions Research Engineering Lab 03755
ATTN: Library

ETL, ATTN: Library 22060

Waterways Experiment Station 39180
ATTN: Library

HQ, XVIII Airborne Corps and Ft. Bragg 28307
ATTN: AFZA-FE-EE

Chanute AFB, IL 61868
3345 CES/DE, Stop 27

Norton AFB 92409
ATTN: AFRCE-MX/DEE

NCEL 93041
ATTN: Library (Code L08A)

Tyndall AFB, FL 32403
AFESC/Engineering & Service Lab

Defense Technical Info. Center 22314
ATTN: DDA (12)

Engineering Societies Library 10017
New York, NY

National Guard Bureau 20310
Installation Division

US Government Printing Office 22304
Receiving Section/Depository Copies (2)

EMS Team Distribution

Chief of Engineers 20314
ATTN: DAEN-MPZ-A
ATTN: DAEN-MPO-B
ATTN. DAEN-MPO-U

US Army Engineer District
New York 10007
ATTN: Chief, Design Br.
Pittsburgh 15222
ATTN: Chief, Engr Div
Philadelphia 19106
ATTN: Chief, NAPEN-D
Baltimore 21203
ATTN: Chief, Engr Div
Norfolk 23510
ATTN: Chief, NAOEN-M
ATTN: Chief, NAOEN-D
Huntington 25721
ATTN: Chief, ORHED-D
Wilmington 28401
ATTN: Chief, SAWEN-DS
ATTN: Chief, SAWEN-D
Charleston 29402
ATTN: Chief, Engr Div
Savannah 31402
ATTN: Chief, SASAS-L
Jacksonville 32232
ATTN: Const Div
ATTN: Design Br., Structures Sec.
Mobile 36628
ATTN: Chief, SAMEN-D
ATTN: Chief, SAMEN-C
Nashville 37202
ATTN: Chief, ORNED-D
Memphis 38103
ATTN: Chief, LMMED-DT
ATTN: Chief, LMMED-DM
Vicksburg 39180
ATTN: Chief, Engr Div
Louisville 40201
ATTN: Chief, Engr Div
Detroit 48231
ATTN: Chief, NCEED-T
St. Paul 55101
ATTN: Chief, ED-D
Chicago 60604
ATTN: Chief, NCCED-DS
Rock Island 61201
ATTN: Chief, Engr Div
ATTN: Chief, NCRED-D
St. Louis 63101
ATTN: Chief, ED-D
Kansas City 64106
ATTN: Chief, Engr Div
Omaha 68102
ATTN: Chief, Engr Div
New Orleans 70160
ATTN: Chief, LMNED-DG
Little Rock 72203
ATTN: Chief, Engr Div
Tulsa 74102
ATTN: Chief, Engr Div
Fort Worth 76102
ATTN: Chief, SWFED-D
Galveston 77550
ATTN: Chief, SWGAS-L
ATTN: Chief, SWGED-DS
ATTN: Chief, SWGED-DM
Albuquerque 87103
ATTN: Chief, Engr Div
Los Angeles 90053
ATTN: Chief, SPLED-D
San Francisco 94105
ATTN: Chief, Engr Div
Sacramento 95814
ATTN: Chief, SPKED-D
Far East 96301
ATTN: Chief, Engr Div
Portland 97208
ATTN: Chief, DB-6
ATTN: Chief, DB-3

US Army Engineer District
Seattle 98124
ATTN: Chief, NPSCO
ATTN: Chief, EN-DB-EM
ATTN: Chief, EN-DB-ST
ATTN: Chief, NPSEN-PL-WC
Walla Walla 99362
ATTN: Chief, Engr Div
Alaska 99501
ATTN: Chief, NPASA-R

US Army Engineer Division
New England 02154
ATTN: Chief, NEDED-T
Middle East (Rear) 22601
ATTN: Chief, MEDED-T
North Atlantic 10007
ATTN: Chief, NADEN-T
South Atlantic 30303
ATTN: Chief, SADEN-TS
ATTN: Chief, SADEN-TE/TM
Huntsville 35807
ATTN: Chief, HNDED-CS
ATTN: Chief, HNDED-ME
ATTN: Chief, HNDED-SR
ATTN: Chief, HNDED-FD
Ohio River 45201
ATTN: Chief, Engr Div
North Central 60605
ATTN: Chief, Engr Div
Missouri River 68101
ATTN: Chief, MRDED-T
Southwestern 75202
ATTN: Chief, SWDED-TS
ATTN: Chief, SWDED-TM
South Pacific 94111
ATTN: Chief, SPDED-TG
Pacific Ocean 96858
ATTN: Chief, Engr Div
ATTN: Chief, FM&S Branch
ATTN: Chief, PODED-D
North Pacific 97208
ATTN: Chief, Engr Div

6th US Army 94129
ATTN: AFKC-EN

7th US Army 09407
ATTN: AETTM-HRD-EHD

HQ, Combined Field Army (ROK/US) 96359
ATTN: CFAR-EN

US Army Foreign Science & Tech. Center
ATTN: Charlottesville, VA 22901
ATTN: Far East Office 96328

USA Liaison Detachment 10007
ATTN: Library

USA ARRADCOM 07801
ATTN: ORDAR-LCA-OK

CERCOM, Ft. Monmouth 07703
ATTN: DRSEL-LE-SS

Defense Nuclear Agency 20305
ATTN: DNA-RAEE
ATTN: DNA-STRA
ATTN: DNA-DDST
ATTN: DNA-RAEV

SHAPE 09055
Chief, Land & Msl. Instl. Section

Ft. Belvoir, VA 22060
ATTN: Learning Resources Center
ATTN: ATSE-TD-TL (2)

Fort Clayton, Canal Zone 34004
ATTN: DFAE

Ft. Leavenworth, KS 66027
ATTN: ATZLCA-SA

Ft. Lee, VA 23801
ATTN: DRXMC-D (2)

Ft. McPherson, GA 30330
ATTN: AFEN-CD

Ft. Monroe, VA 23651
ATTN: ATEN-AD (3)
ATTN: ATEN-FE-BG (2)
ATTN: ATEN-FE-W

Aberdeen Proving Ground, MD 21005
ATTN: AMXHE

Harry Diamond Labs 20783
ATTN: DELHD-NW-E
ATTN: DELHD-NW-EA
ATTN: DELHD-NW-EC
ATTN: DELHD-NW-ED
ATTN: DELHD-NW-EE

USA Natick Labs 01760
NARADCOM/DRDNA-UST

USA-WES 39180
ATTN: C/Structures

NAVFAC/Code 04
Alexandria, VA 22332

Naval Air Systems Command 20360
ATTN: Library

Naval Training Equipment Command 32813
ATTN: Technical Library

Port Hueneme, CA 93043
ATTN: Morell Library

Bolling AFB, DC 20332
AF/LEEEU

AFE, Camp Humphreys
APO San Francisco 96721

Griffiss AFB 13440
RADC/RBES

Hanscom AFB, MA 01731
ATTN: HQ AFSC
ATTN: ESD/OCR-3

Kirtland AFB, NM 87117
ATTN: AFWL/DES
ATTN: AFWL/DYC

Little Rock AFB 72076
ATTN: 314/DEEE

Patrick AFB, FL 32925
ATTN: XRQ

Tinker AFB, OK 73145
2854 ABG/DEEE

Tyndall AFB, FL 32403
ATTN: AFESC/TBT
ATTN: AFESC/RDCF

Wright-Patterson AFB, OH 45433
ATTN: ASD/ENAMA
ATTN: AFWAL/MLSE

Bldg. Research Advisory Board 20418
Dept. of Transportation Library 20590
Transportation Research Board 20418

Airports and Const. Services Dir.
Technical Info. Reference Centre
Ottawa, Canada K1A ON8

Axford, Roy A.
Evaluation of the applicability of standard CW EMI/RFI shielding effectiveness test techniques to the assessment of the EMP hardness of tactical shelters / by Roy Axford, Ray McCormack, Raj Mittra. -- Champaign, IL : Construction Engineering Research Laboratory ; available from NTIS, 1982
57 p. (Technical report ; M-307)

1. Electromagnetic interference 2. Shielding (electricity) I. McCormack, Raymond G. II. Mittra, Raj. III. Title. IV. Series : U. S. Army. Construction Engineering Research Laboratory. Technical report ; M-307.